Electronic Supplementary Material (ESI) for Dalton Transactions.

Supporting information for

CFA-18: A homochiral metal–organic framework (MOF) constructed from rigid enantiopure bistriazolate linker molecules

Katharina Knippen[a], Björn Bredenkötter[a], Lisa Kanschat[a], Maryana Kraft[a], Tom Vermeyen[b,d], Wouter Herrebout[b], Kunihisa Sugimoto[c], Patrick Bultinck[d] and Dirk Volkmer*[a]

Corresponding author: Prof. Dr. Dirk Volkmer
E-mail: dirk.volkmer(at)physik.uni-augsburg.de
Tel.: +49 (0) 821/598-3032
Fax: +49 (0) 821/598-5955

Table of content:

1. Analytical data:

1.1: 3,3,3',3'-tetramethyl-2,2',3,3'-tetrahydro-1,1'-spirobi[indene]-6,6'-diol (rac-1) and (aR-1)

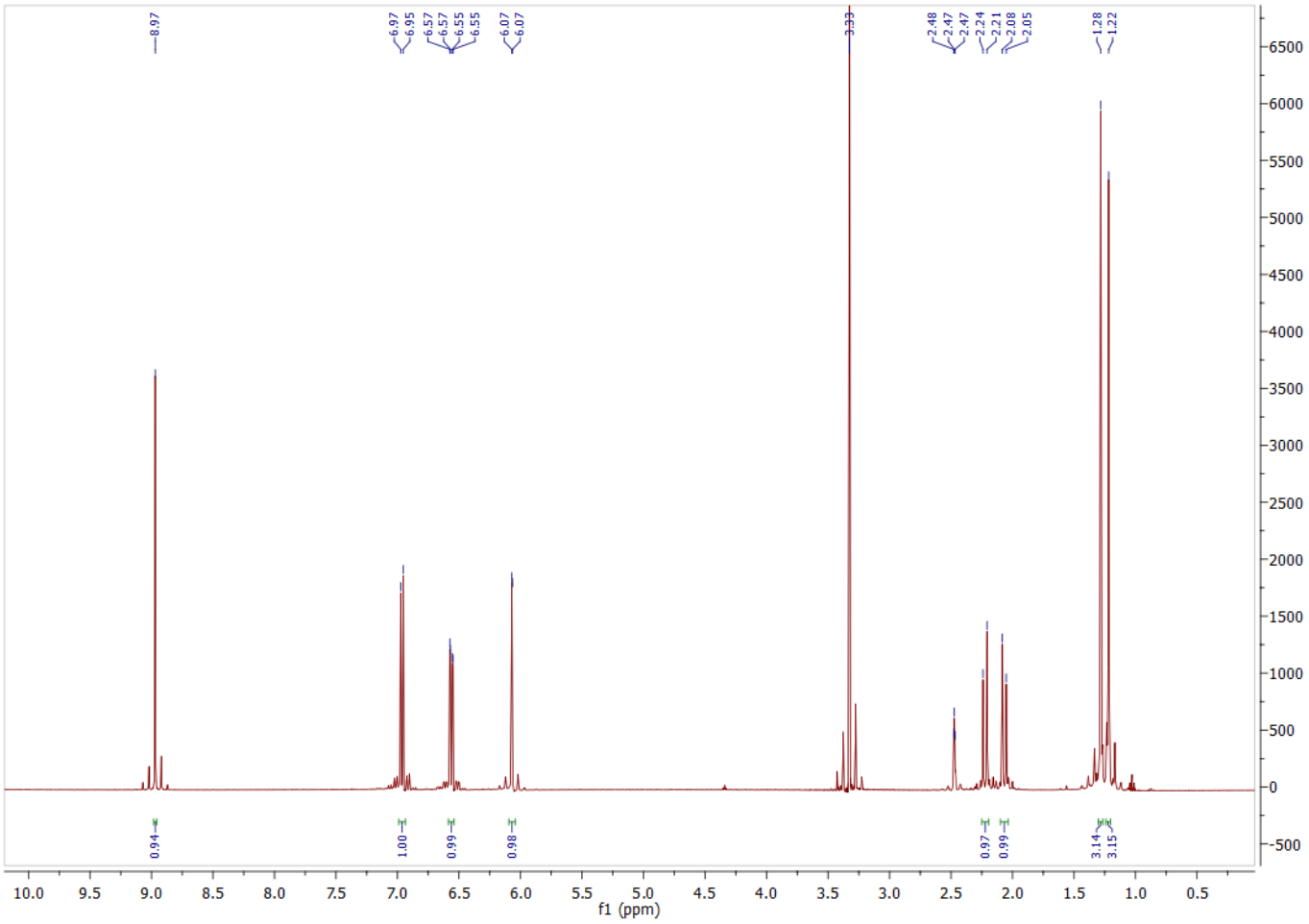

Figure S1: ^{1}H NMR of *rac*- and *aR*-**1** (400 MHz, d_6-DMSO, 20°C).

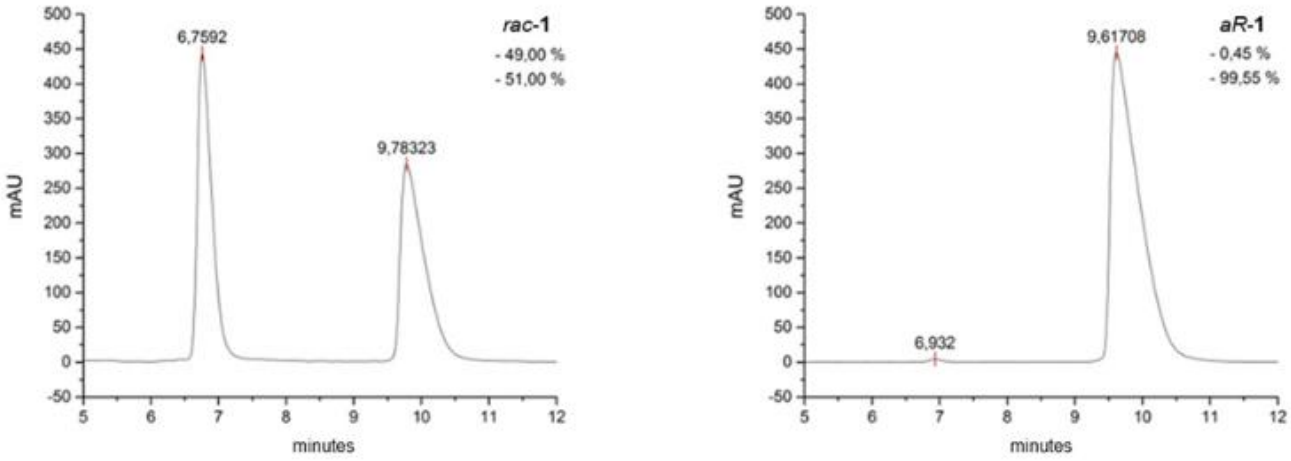

Figure S2: HPLC (left: rac-1, right, aR-1; flow rate: 1 ml/min; injection volume: 20 µl and 10 µl).

⇨ ee 99%

1.2: 3,3,3',3'-tetramethyl-2,2',3,3'-tetrahydro-1,1'-spirobi[indene]-6,6'-diyl bis[(1R,2S,5R)-5-menthyl-2-(propan-2-yl)cyclohexyl] biscarbonates (rac-2) and (aR-2)

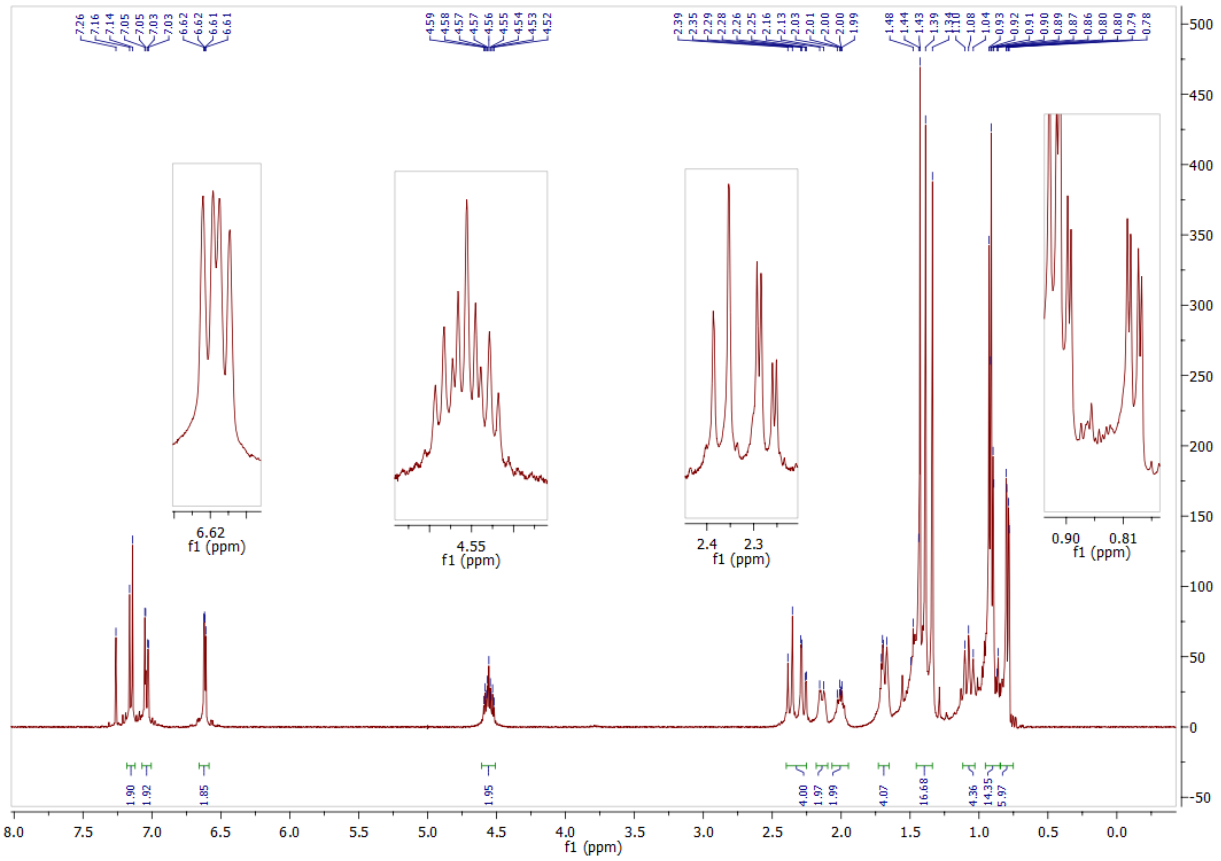

Figure S3: ^{1}H NMR of *rac*-**2** (400 MHz, $CDCl_3$, 20°C).

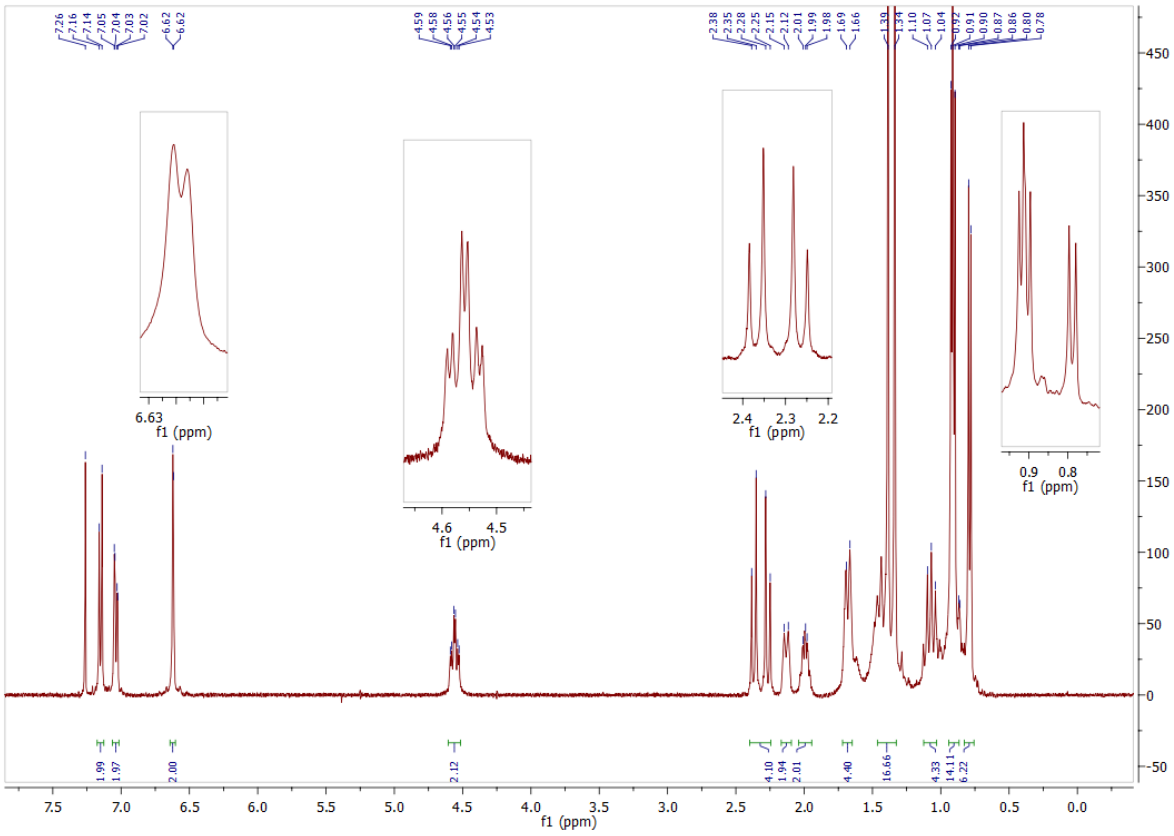

Figure S4: ^{1}H NMR of *aR*-**2** (400 MHz, $CDCl_3$, 20°C).

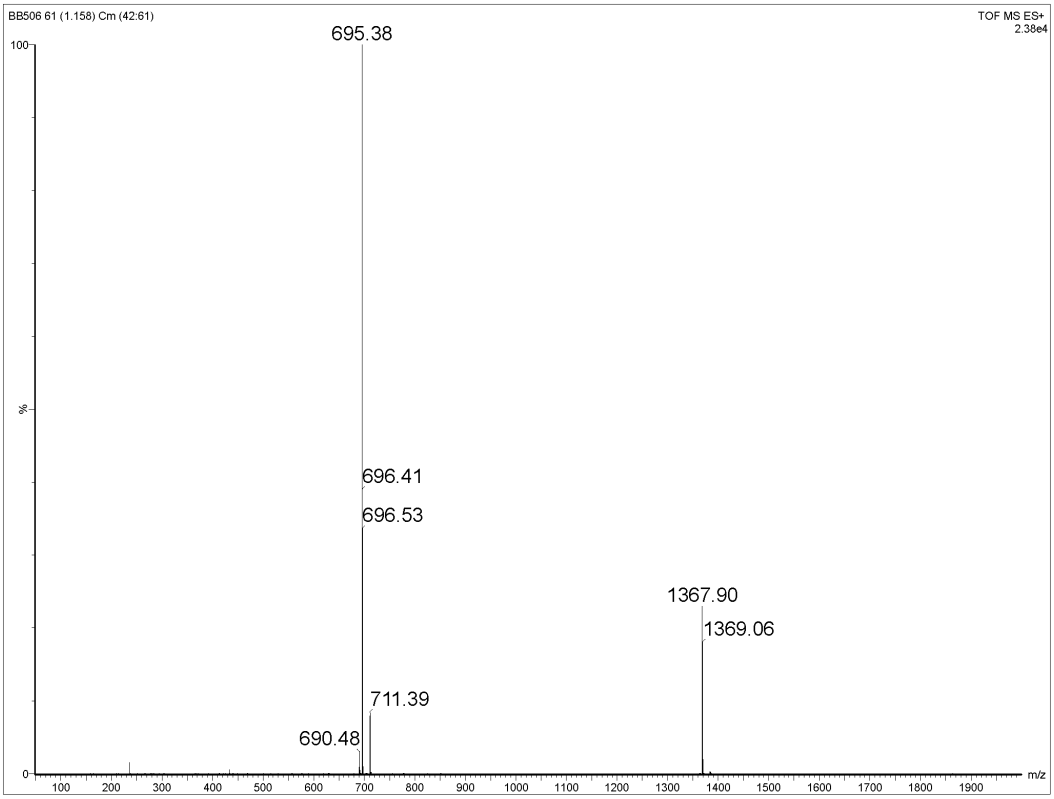

Figure S5: ESI(+)-MS of *aR*-**2**.

1.3: aR-3,3,3',3'-tetramethyl-5,5‘-dinitro-2,2',3,3'-tetrahydro-1,1'-spirobi[indene]-6,6'-diyl bis[(1R,2S,5R)-5-methyl-2-(propan-2-yl)cyclohexyl] biscarbonate (aR-3)

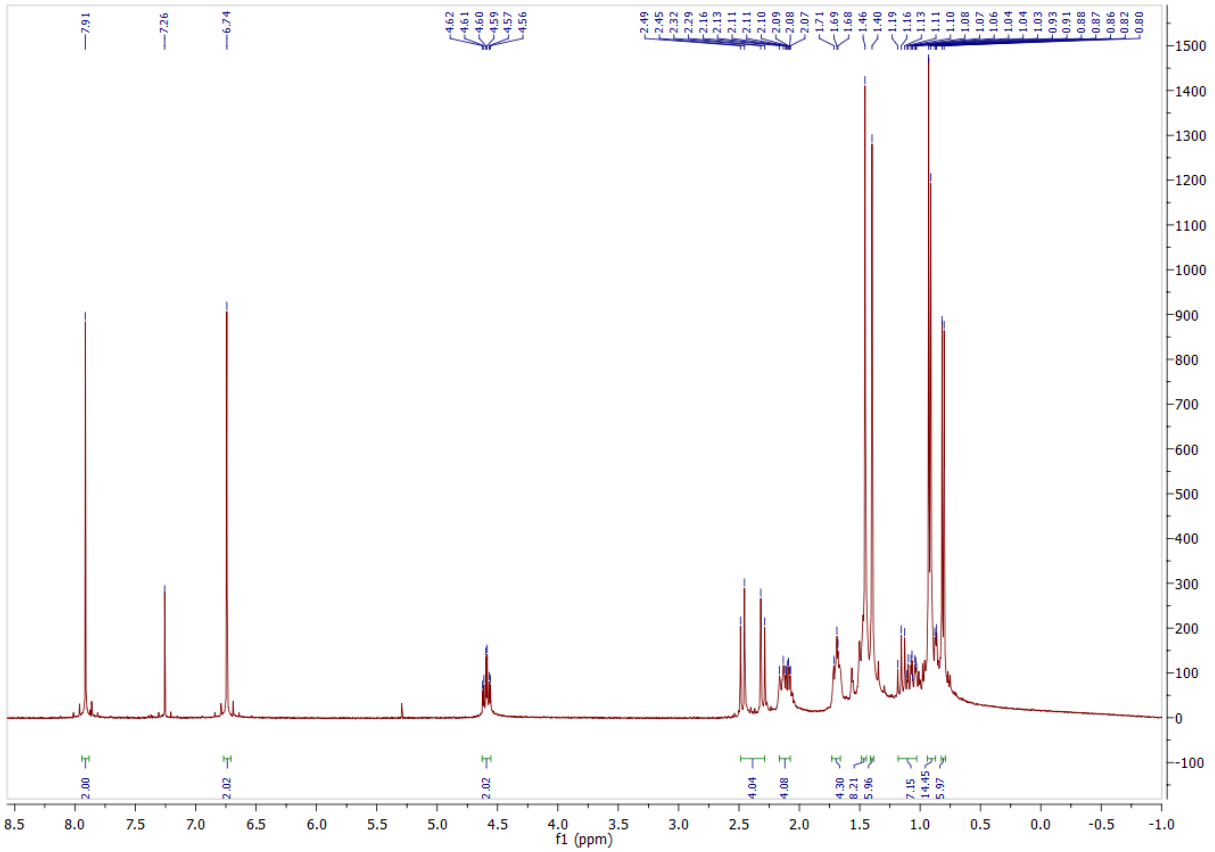

Figure S6: ^{1}H NMR of *aR*-**3** (400 MHz, $CDCl_3$, 20°C).

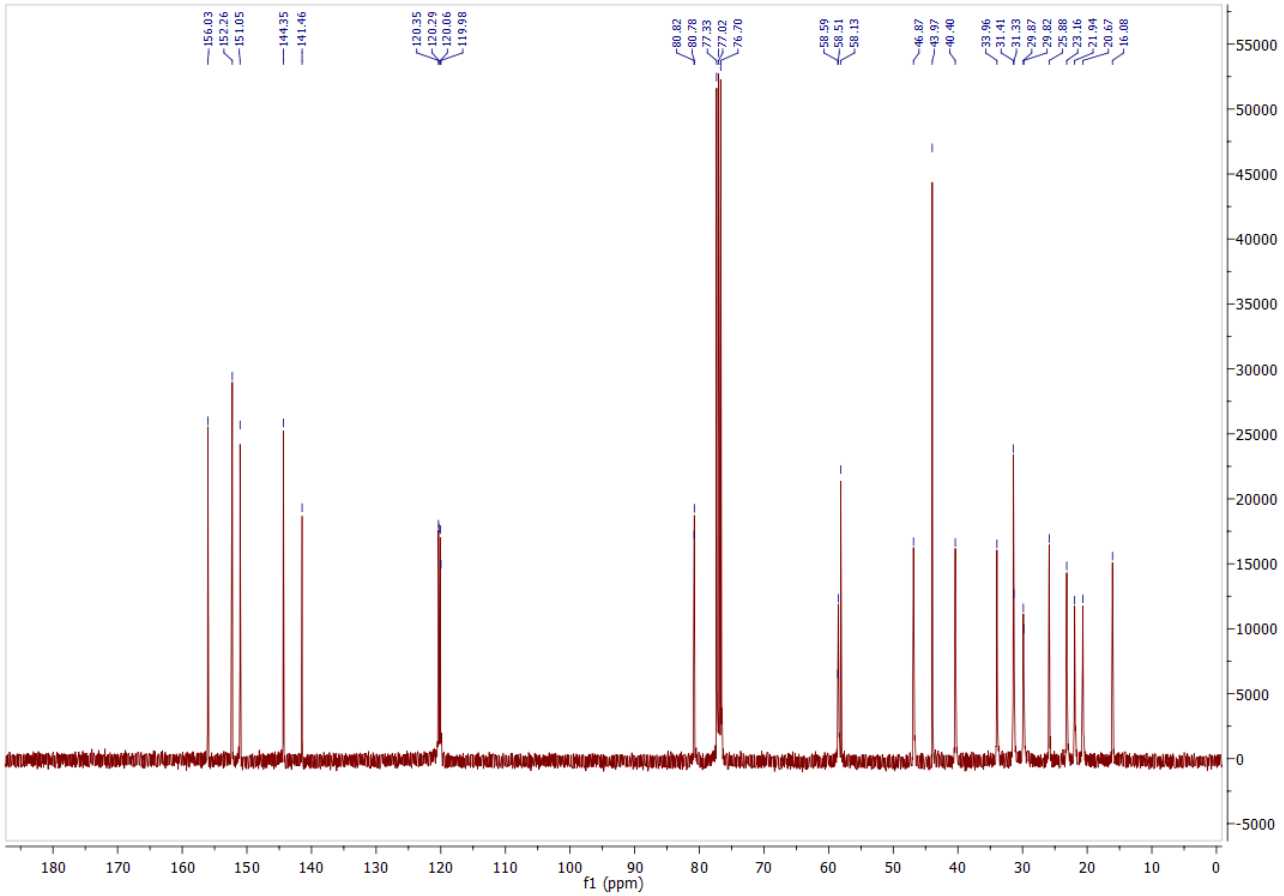

Figure S7: ^{13}C NMR of *aR*-**3** (100 MHz, $CDCl_3$, 20°C).

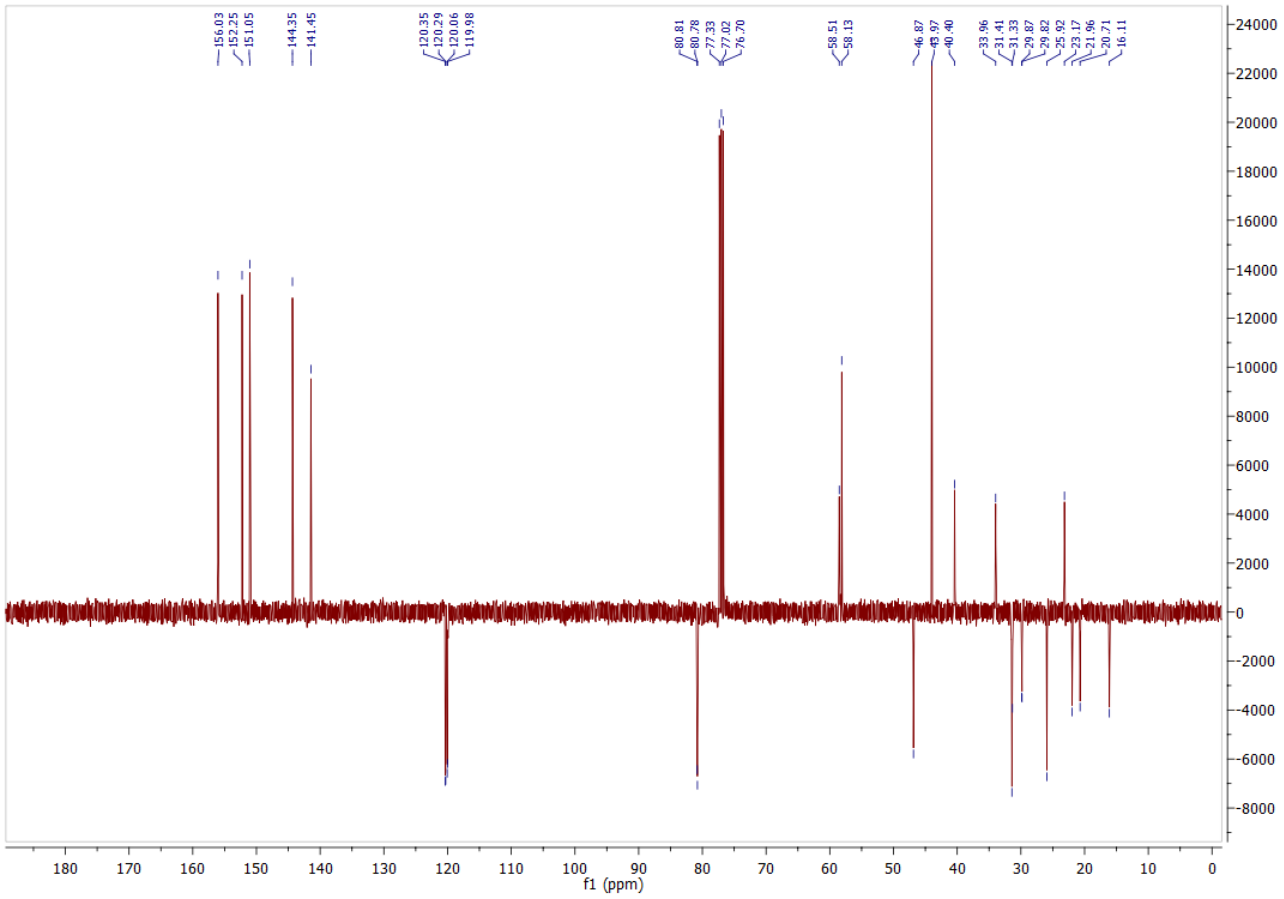

Figure S8:^{13}C-APT NMR of *aR*-**3** (100 MHz, $CDCl_3$, 20°C).

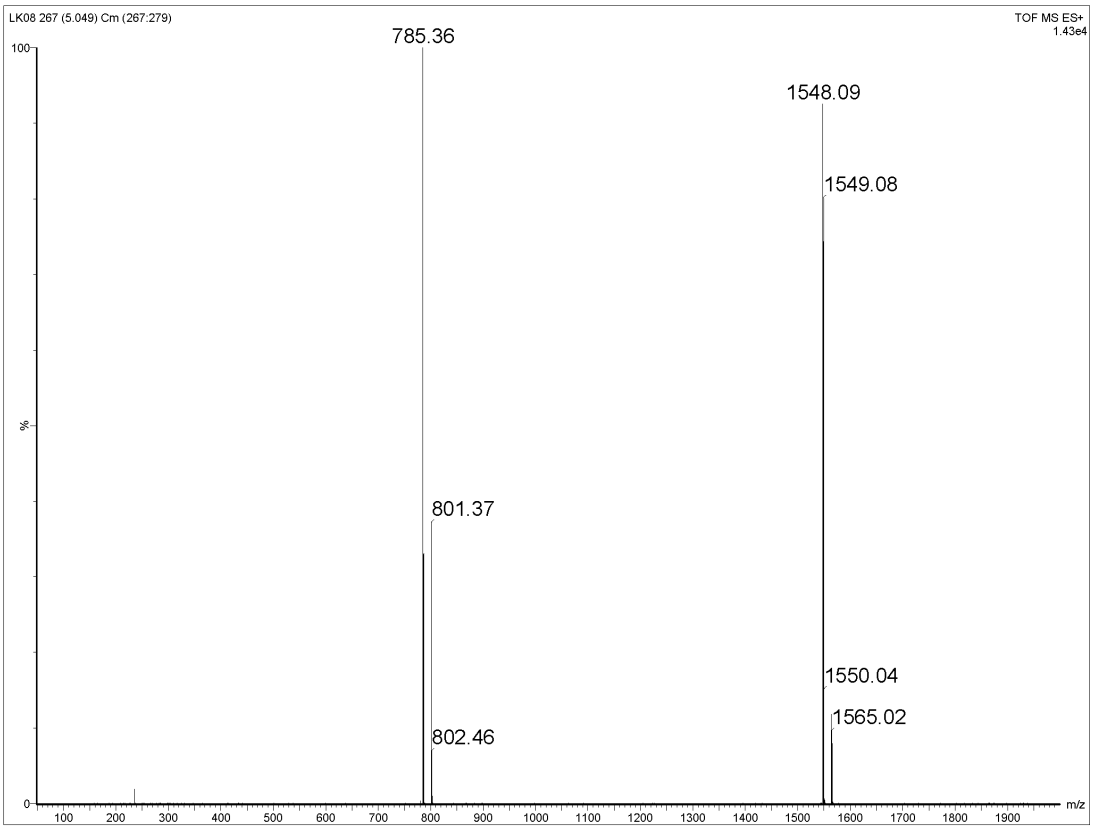

Figure S9: ESI(+)-MS of *aR*-**3**.

1.4: aR-3,3,3',3'-tetramethyl-5,5‘-dinitro-2,2',3,3'-tetrahydro-1,1'-spirobi[indene]-6,6'-diol (aR-4)

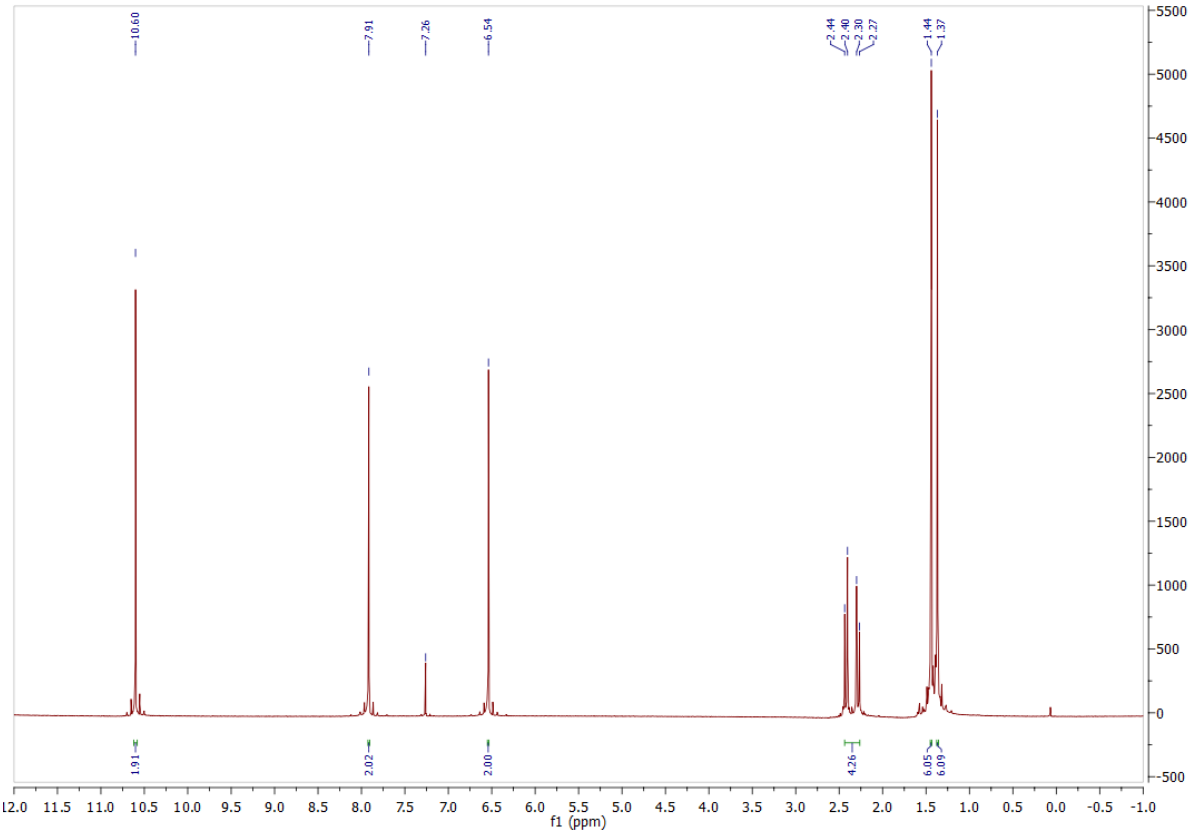

Figure S10: ^{1}H NMR of *aR*-**4** (400 MHz, $CDCl_3$, 20°C).

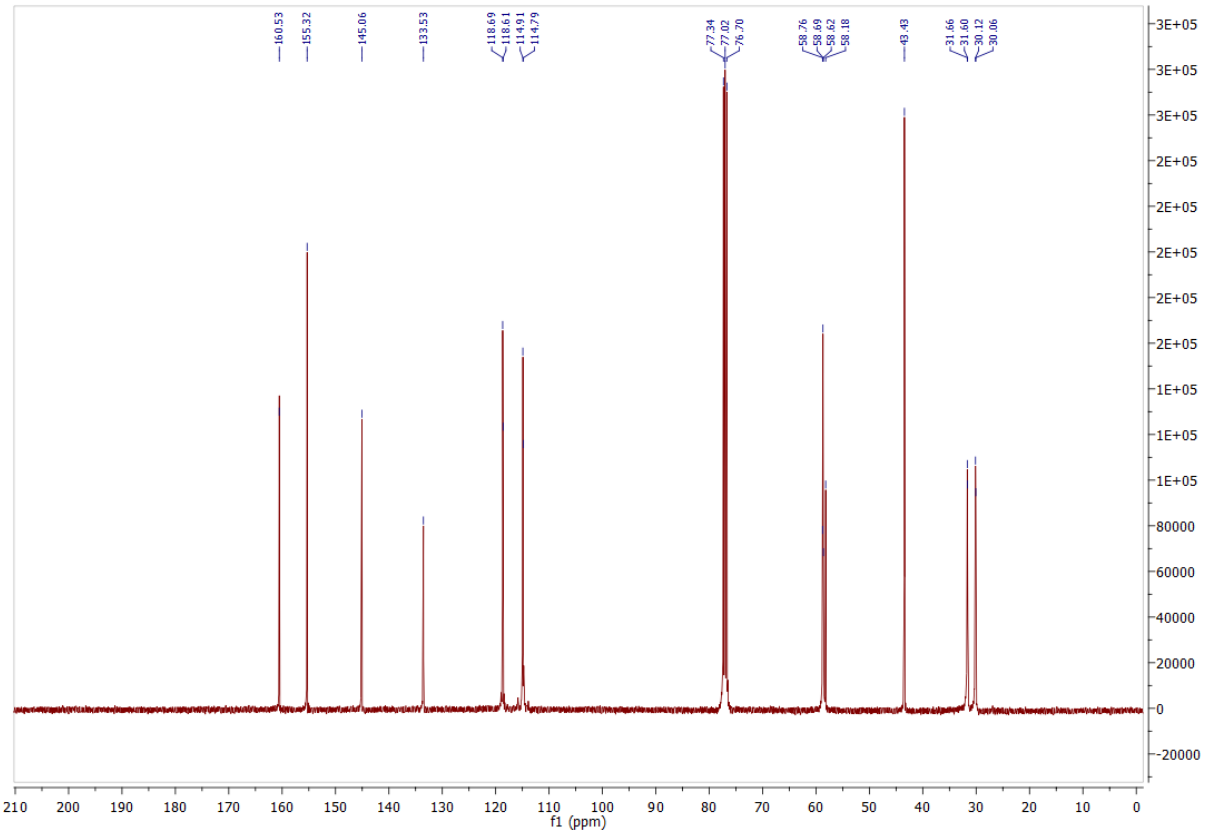

Figure S11: ^{13}C NMR of *aR*-**4** (100 MHz, $CDCl_3$, 20°C).

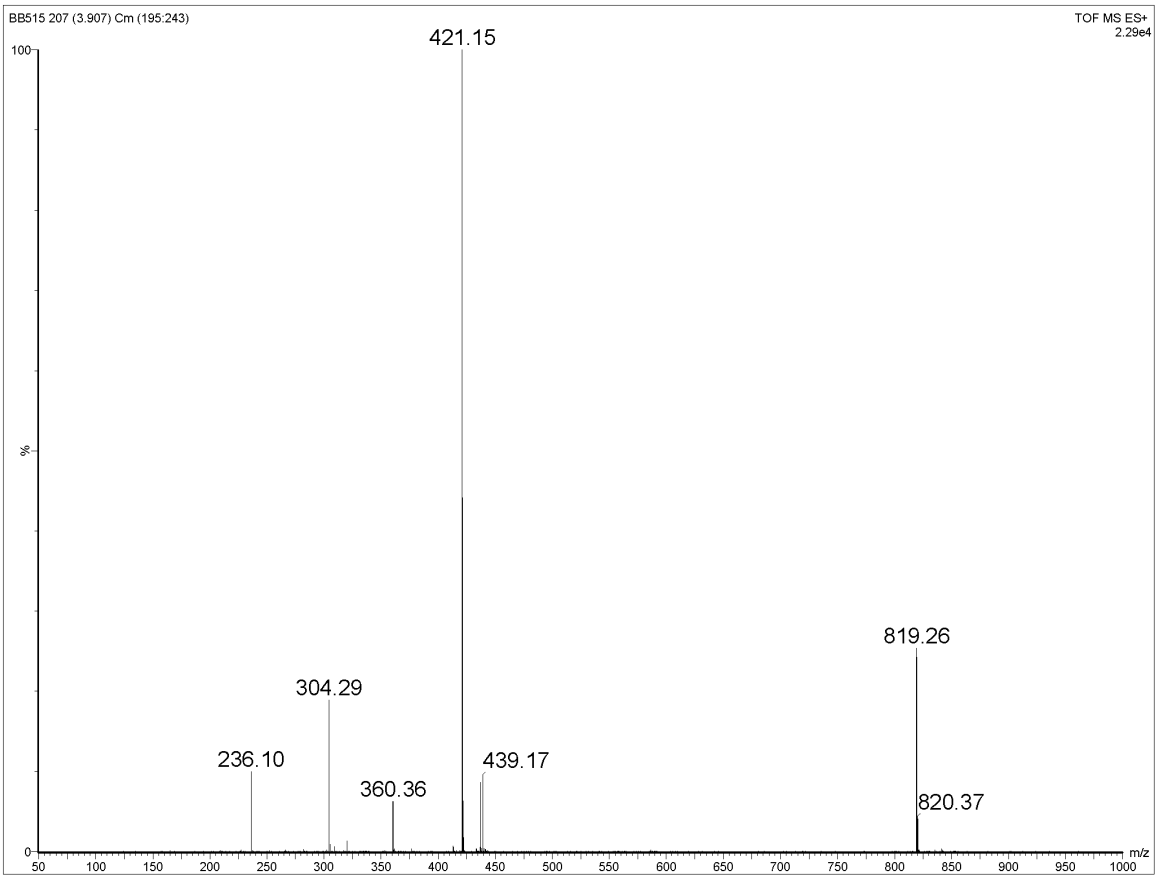

Figure S12: ESI(+)-MS of *aR*-**4**.

1.5: aR-3,3,3',3'-tetramethyl-5,5‘-dinitro-2,2',3,3'-tetrahydro-1,1'-spirobi[indene]-6,6'-diamine (aR-5)

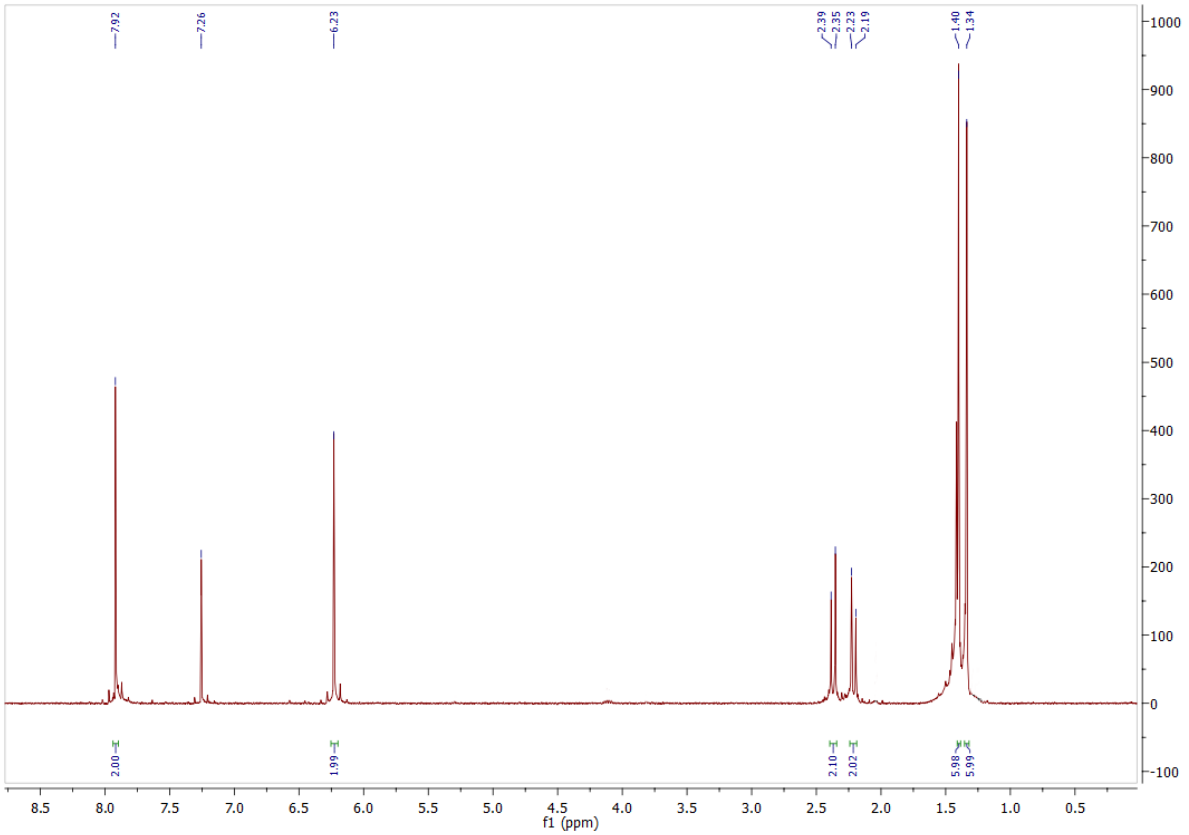

Figure S13.[1]H NMR of *aR*-**5** (400 MHz, $CDCl_3$, 20°C).

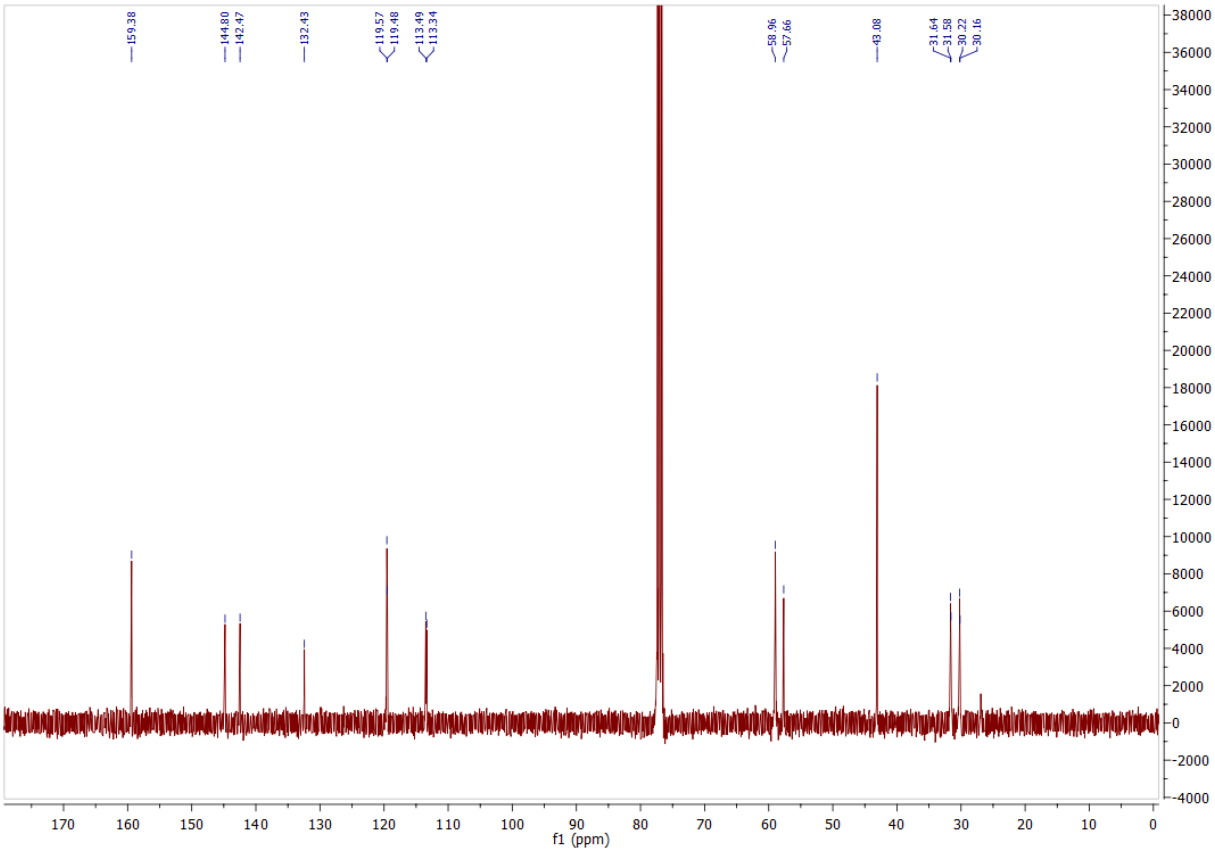

Figure S14: [13]C NMR of *aR*-**5** (100 MHz, $CDCl_3$, 20°C).

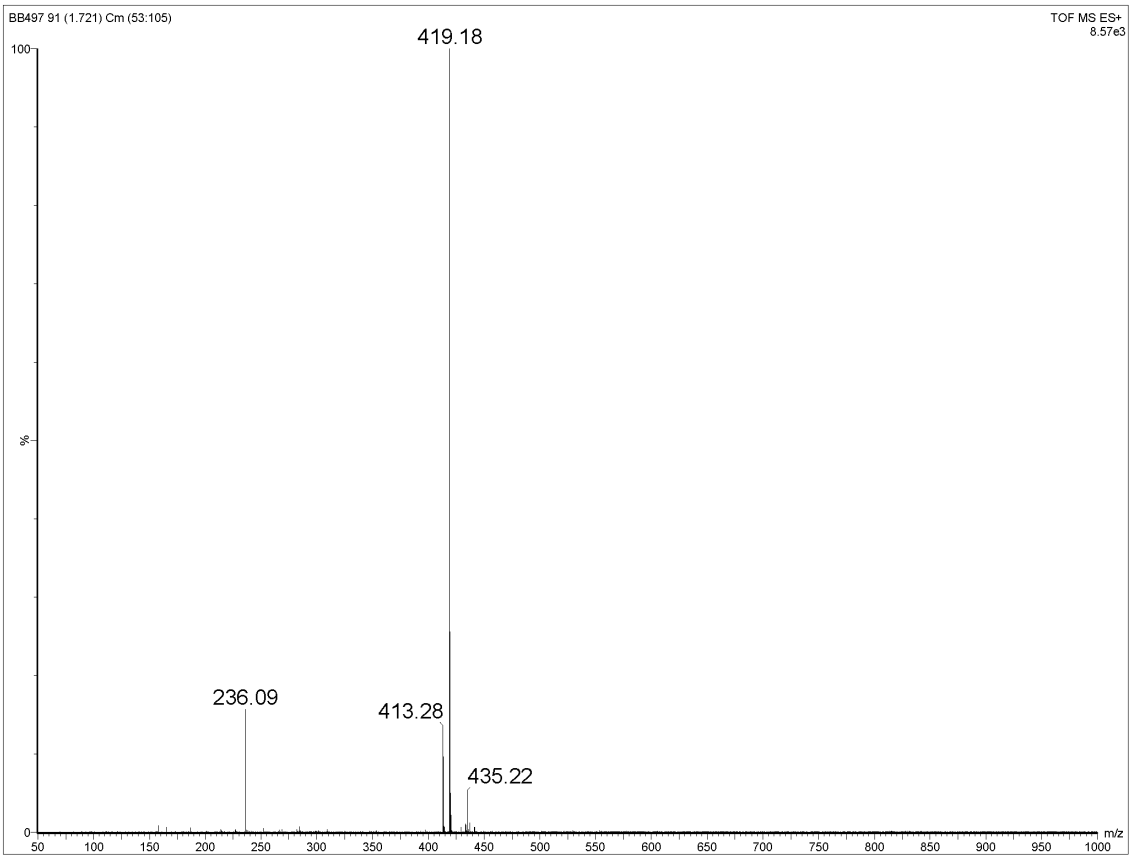

Figure S15: ESI(+)-MS of *aR*-**5**.

1.6: aR-3,3,3',3'-tetramethyl-2,2',3,3'-tetrahydro-1,1'-spirobi[indene]-5,5‘,6,6'-tetraamine (aR-6)

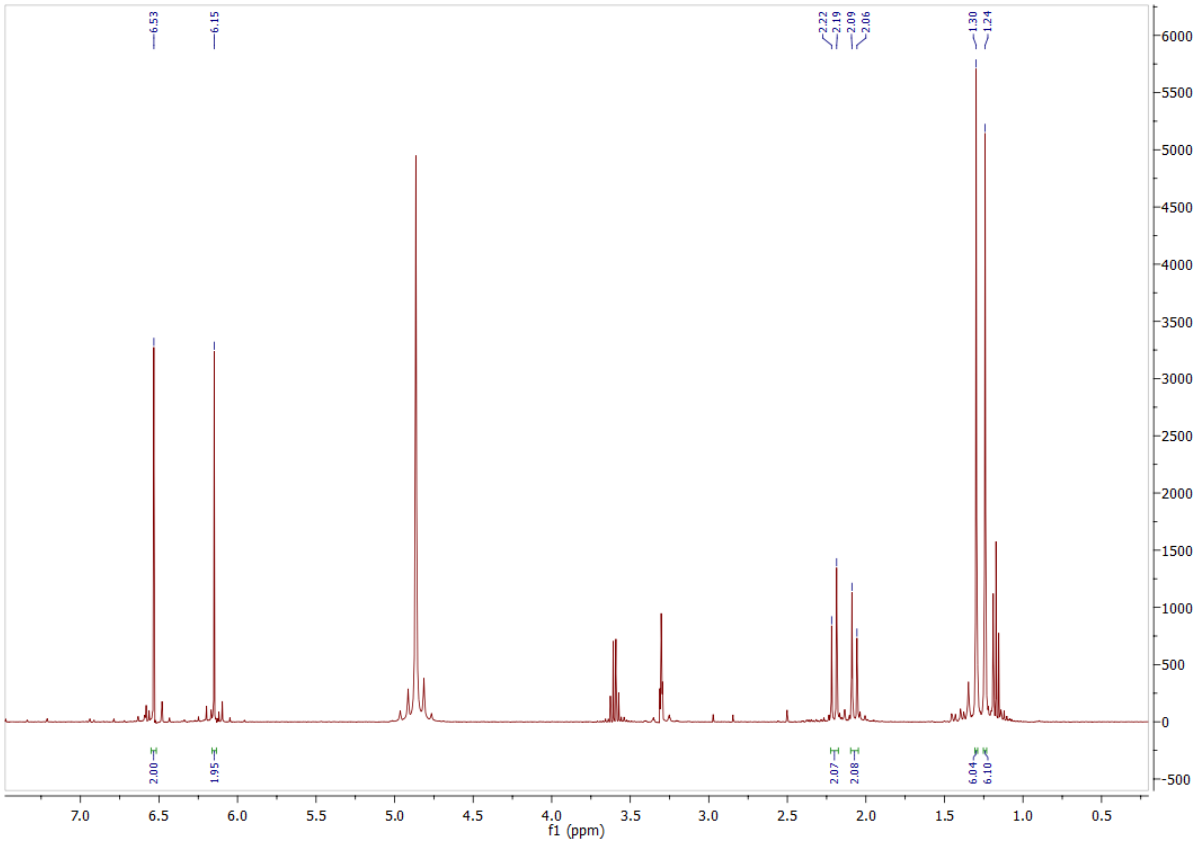

Figure S16: ^{1}H NMR of *aR*-**6** (400 MHz, d_4-methanol, 20°C).

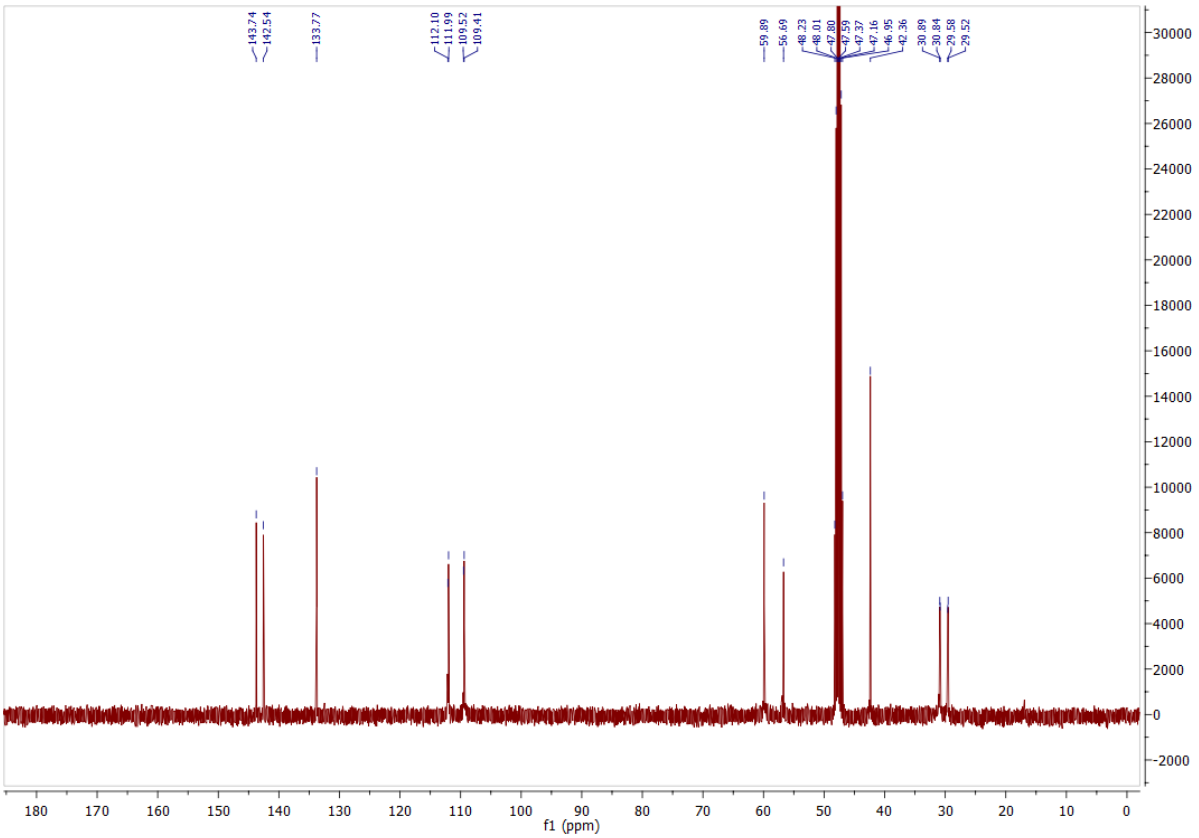

Figure S17: ^{13}C NMR of *aR*-**6** (100 MHz, d_4-methanol, 20°C).

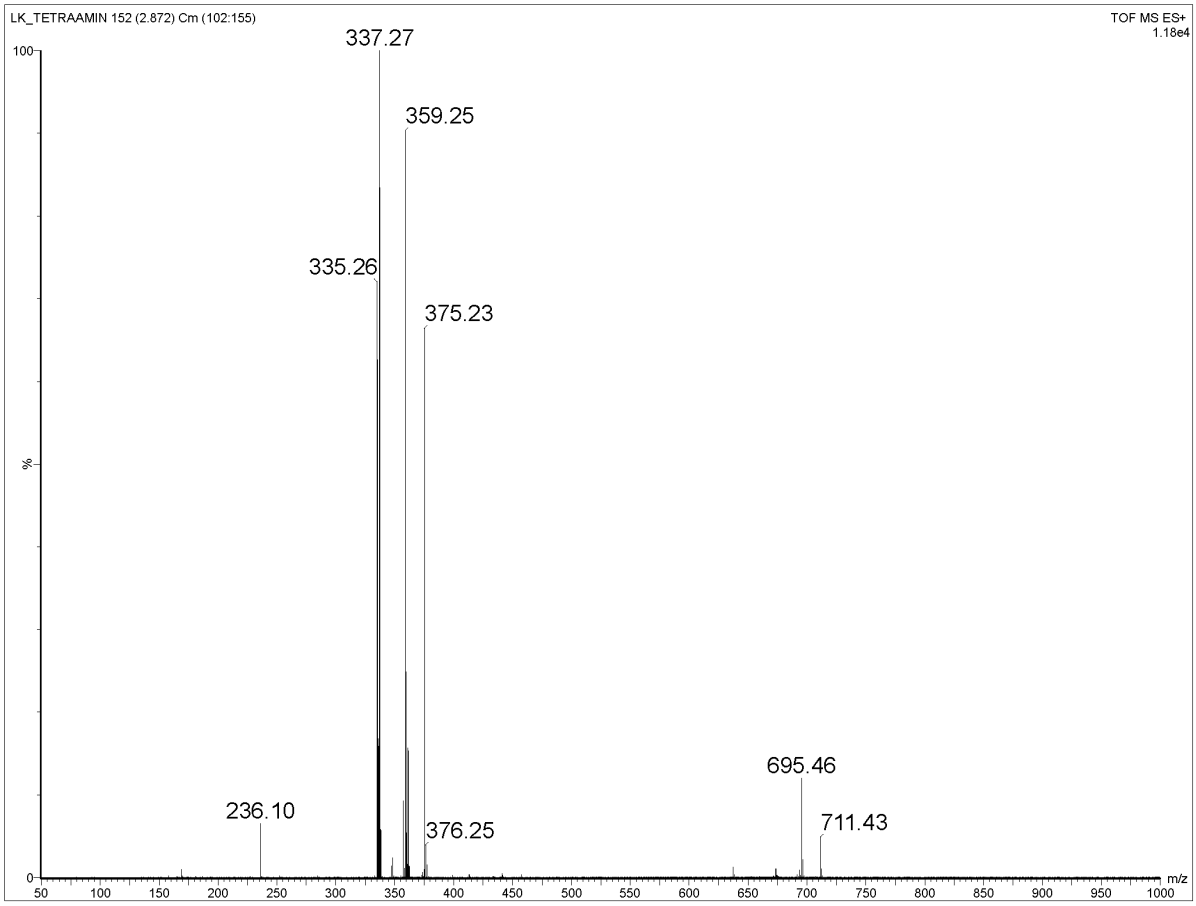

Figure S18: ESI(+)-MS of *aR*-**6**.

1.7: aR-7,7,7',7'-tetramethyl-6,6',7,7'-tetrahydro-1H,3'H-5,5'-spirobi[indeno[5,6-d][1,2,3]triazole] (aR-7)

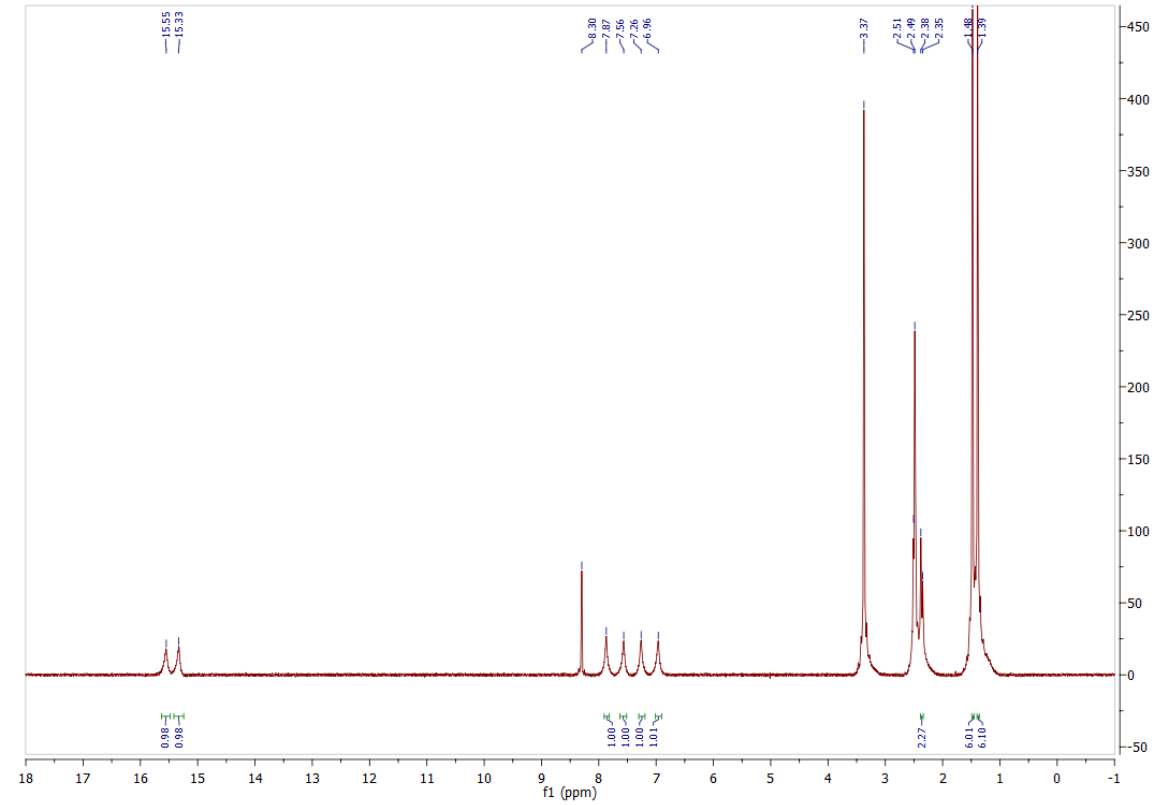

Figure S19: ^{1}H NMR of *aR*-**7** (400 MHz, d_6-DMSO, 20°C).

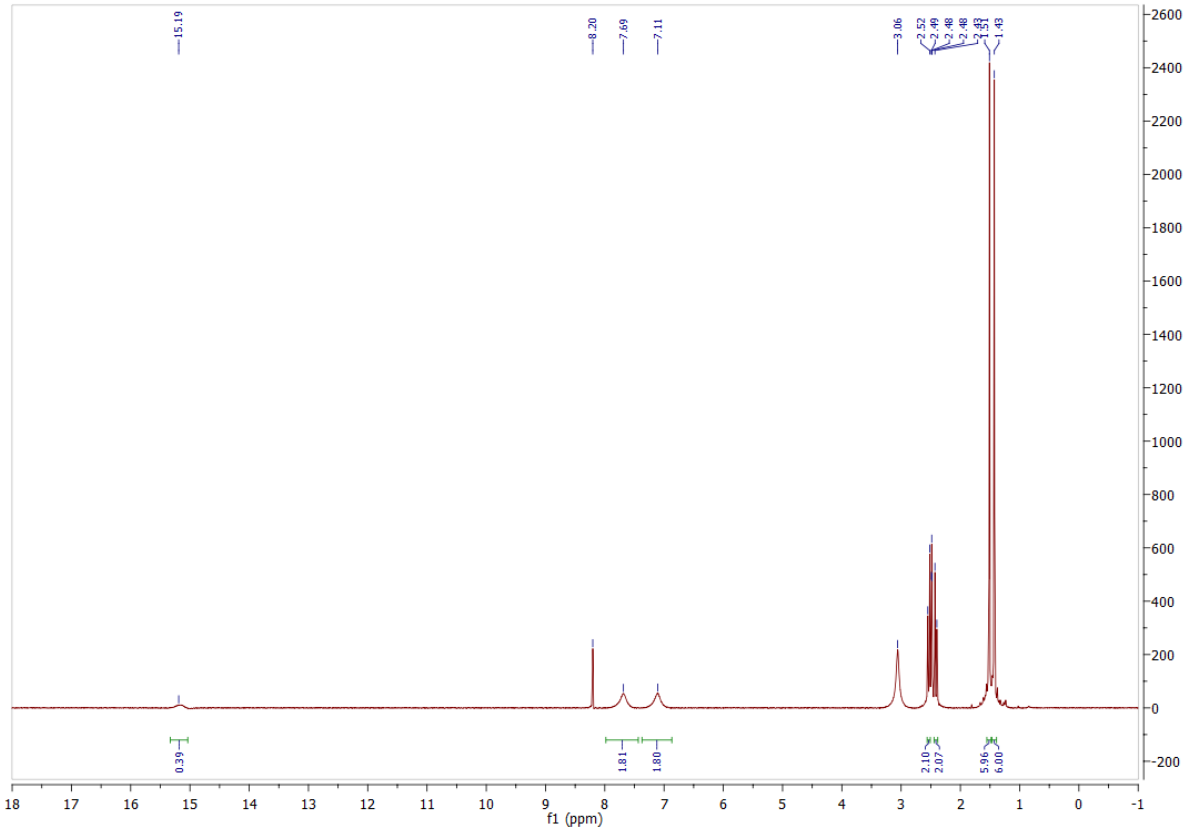

Figure S20: ^{1}H NMR of *aR*-**7** (100 MHz, d_6-DMSO, 80°C).

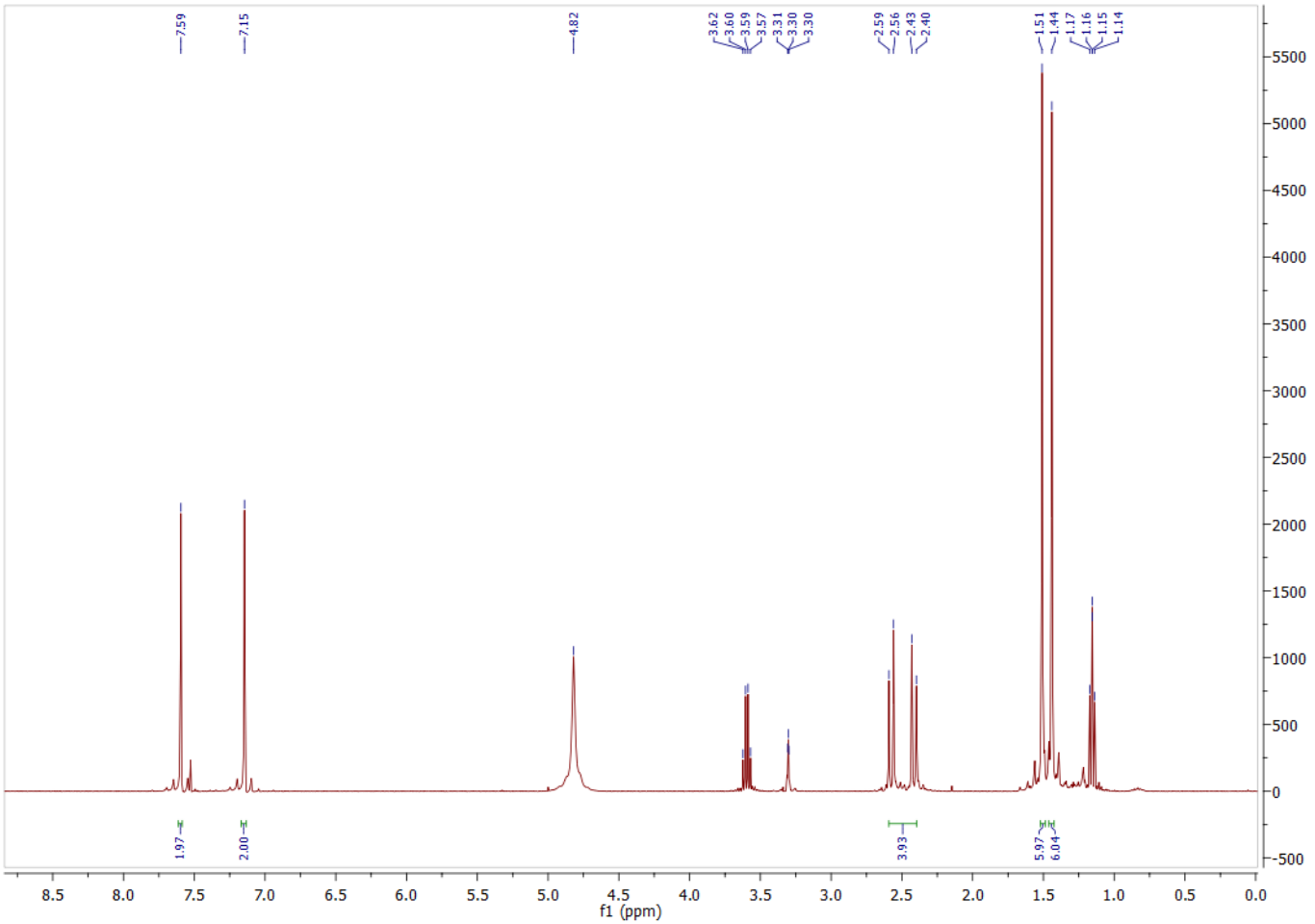

Figure S21: ^{1}H NMR of *aR*-**7** (400 MHz, $CDCl_3$, d_4-methanol 9:1, 20°C).

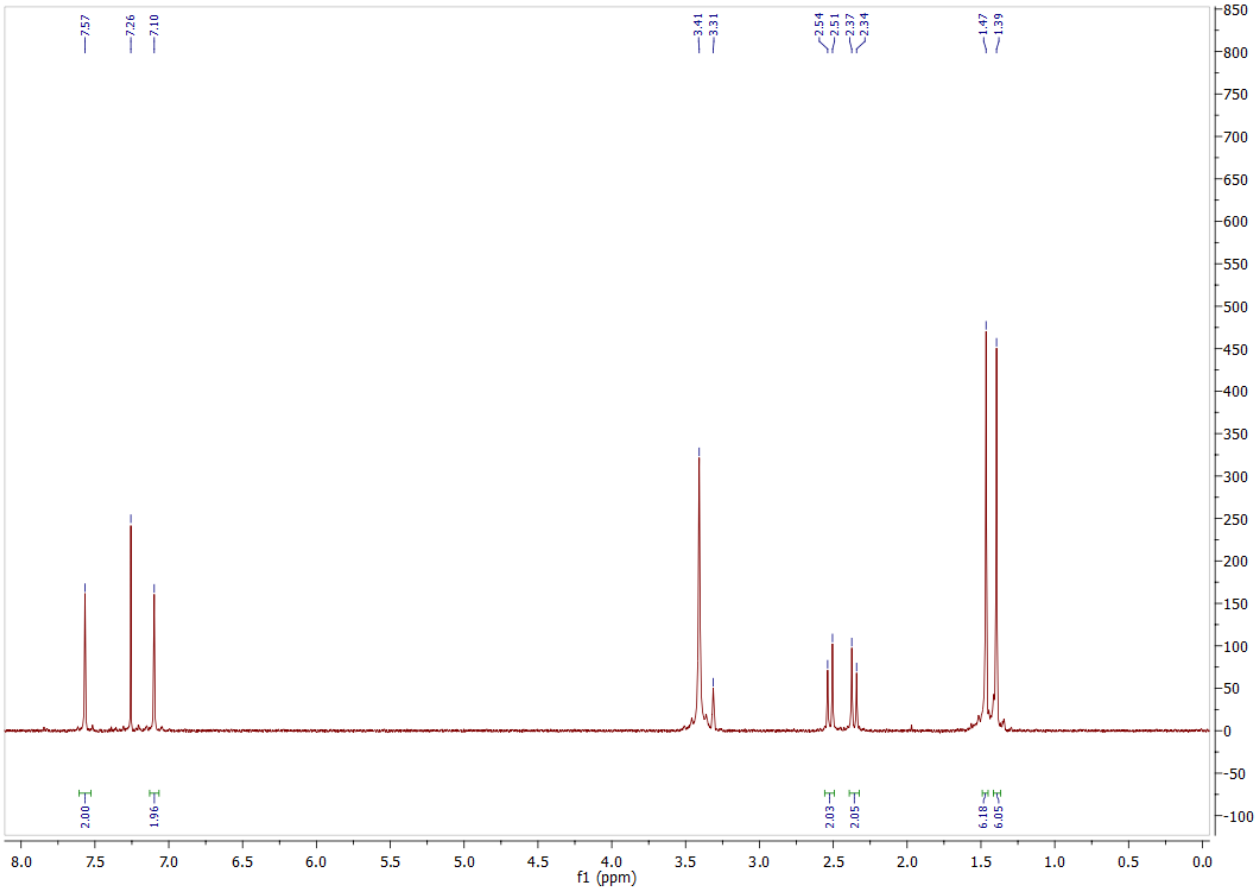

Figure S22: ^{1}H NMR of *aR*-**7** (400 MHz, $CDCl_3$, d_4-methanol 49:1, 20°C).

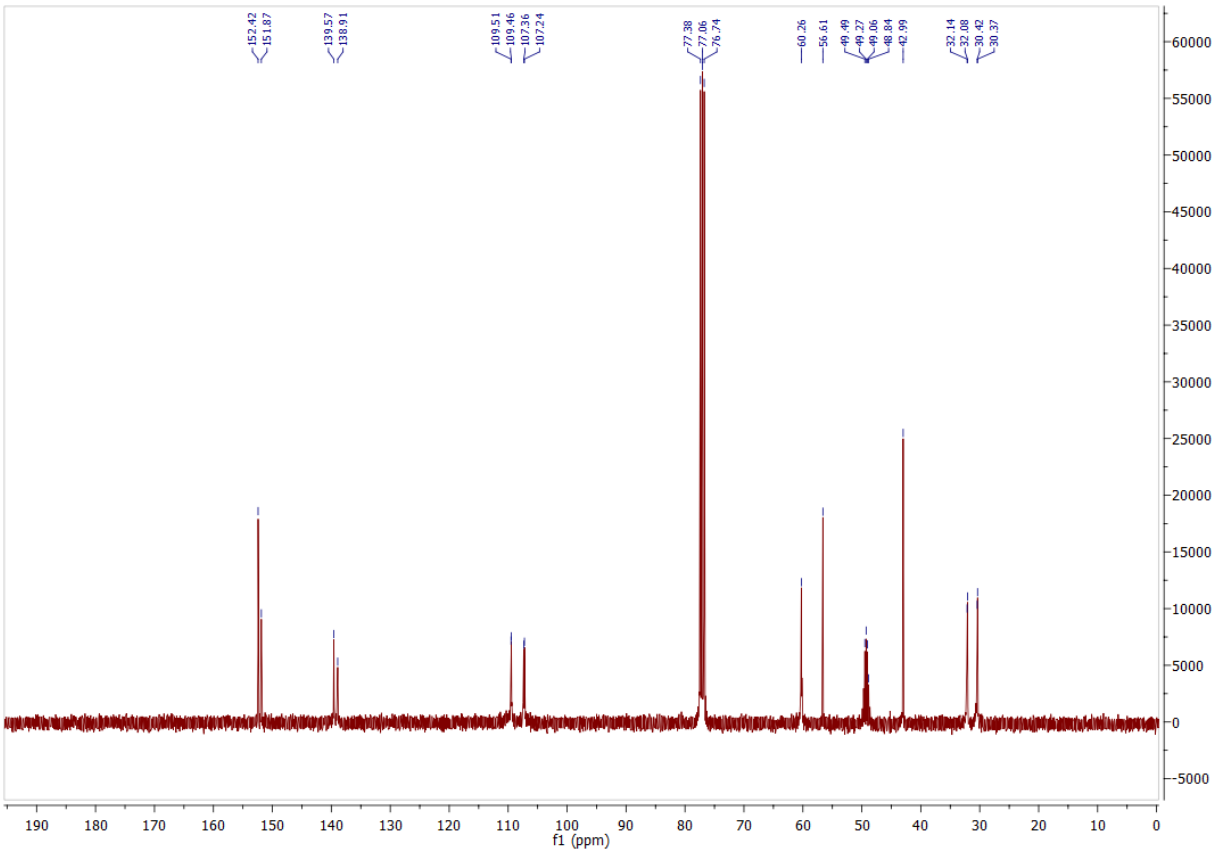

Figure S23: ^{13}C NMR of *aR*-**7** (100 MHz, $CDCl_3$, d_4-methanol 49:1, 20°C).

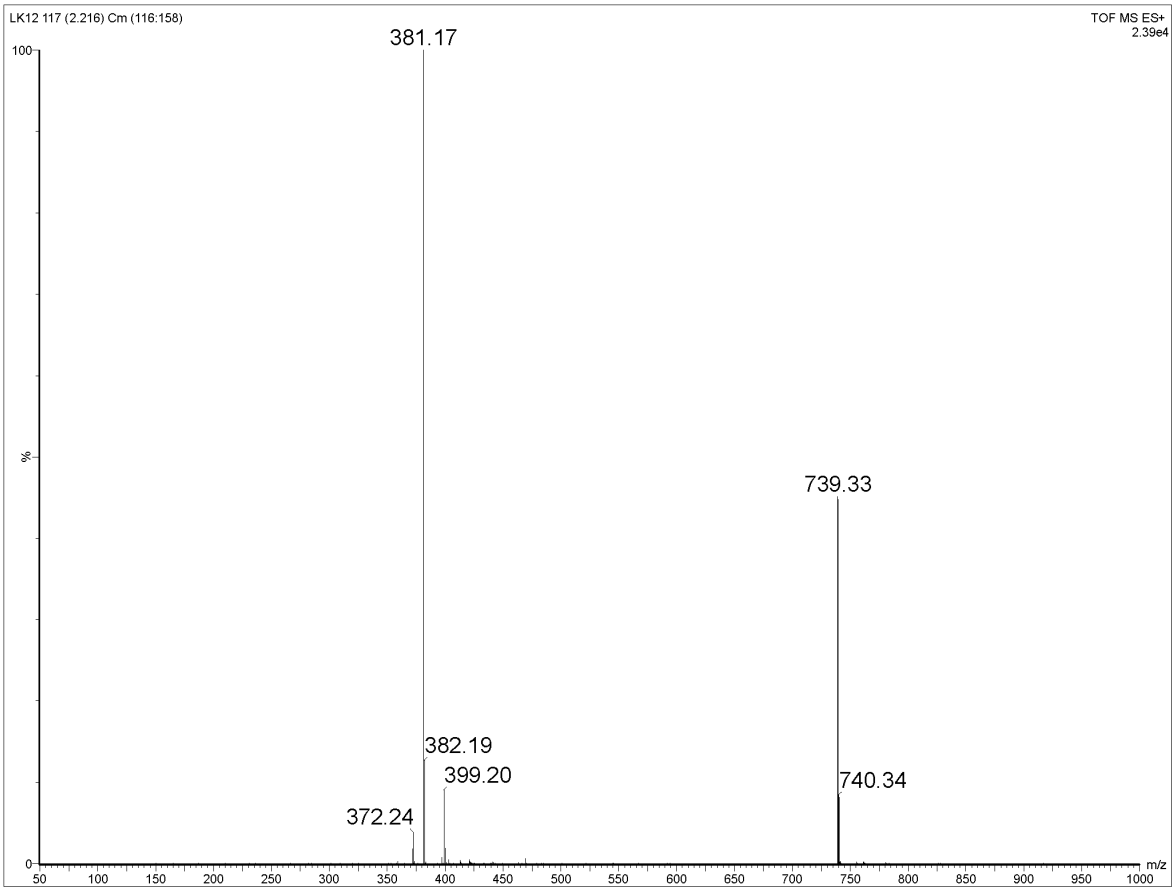

Figure S24:ESI(+)-MS of *aR*-**7**.

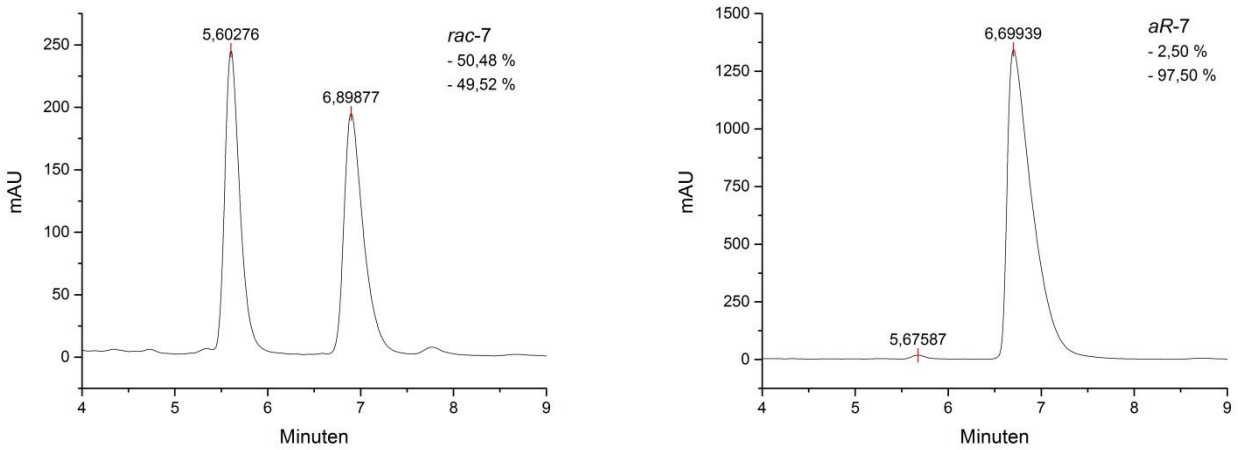

Figure S25: HPLC (left: *rac*-**7**, right, *aR*-**7**; flow rate: 1 ml/min; injection volume: 10 µl and 40 µl).

⇨ ee 95%

2. VCD spectroscopy:

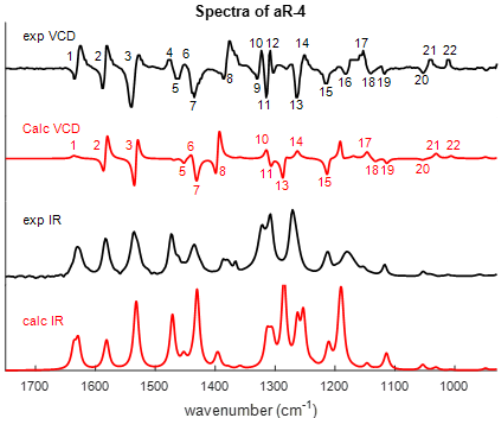

Figure S26: From top to bottom the experimental VCD spectrum, calculated VCD spectrum, experimental IR spectrum and calculated IR spectrum of *aR*-**4**. A global shifting factor of 0.985 was used for the calculated spectra.

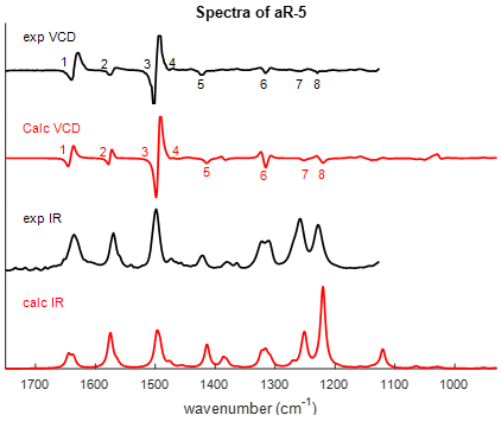

Figure S27:From top to bottom the experimental VCD spectrum, calculated VCD spectrum, experimental IR spectrum and calculated IR spectrum of *aR*-**5**. A global shifting factor of 0.985 was used for the calculated spectra.

3. Verification of the intact linker in CFA-18 via FT-IR and NMR:

In addition to the single crystal X-ray analysis, FT-IR- and NMR- analysis was used to determine the intactness of the build-in linker molecule in **CFA-18**.
The comparison of FT-IR spectra of the pure linker molecule and **CFA-18** in Figure S28 shows a number of IR-bands, having their origin from the organic molecule, but also indicates some clear differences caused by coordination of the linkers to the metal ions of the framework's SBU. The bands caused by the benzotriazol part of *H_2-spirta* (*aR*-**7**) can be certainly assigned. These are for instance the benzyl stretching vibration at 1460 cm^{-1}, the triazol breathing vibrations at 1200 cm^{-1} or the benzyl breathing at 800 cm^{-1} (Figure S 28, green part). In contrast to that, the differences between linker IR-bands and MOF IR-bands are marked with a blue background. For instance, an intensive band at 1658 cm^{-1} is indicating a C=O stretch vibration, which results from the coordinated neutral DMF-ligand and an additional band at 680 cm^{-1} is presumably caused by the Mn-O stretch vibration (Figure S 28, blue background) [1,2,2,3].

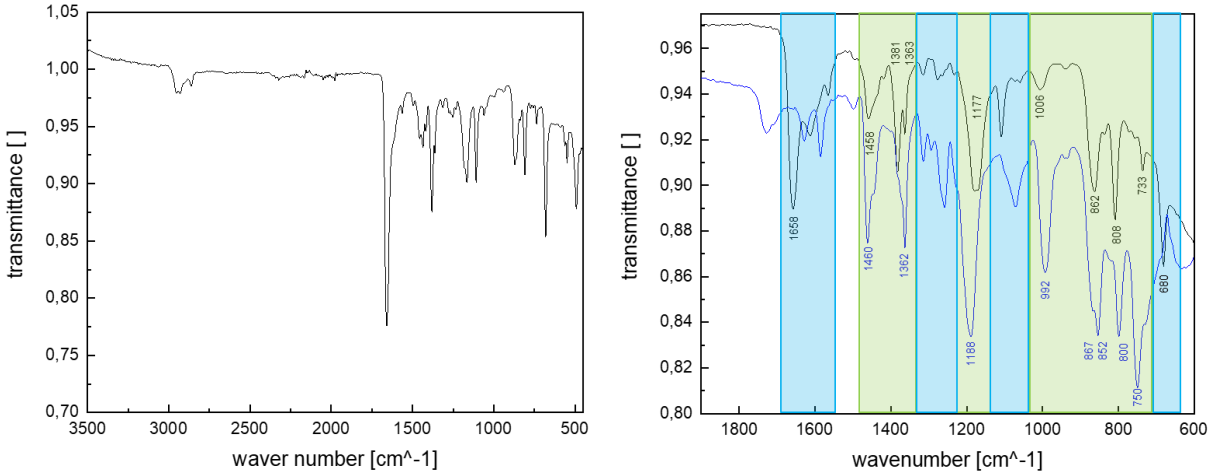

Figure S28: FT-IR spectrum of CFA-18 (left) and the magnification of comparison (right) of CFA-18 (black) with H2-spirta (blue).

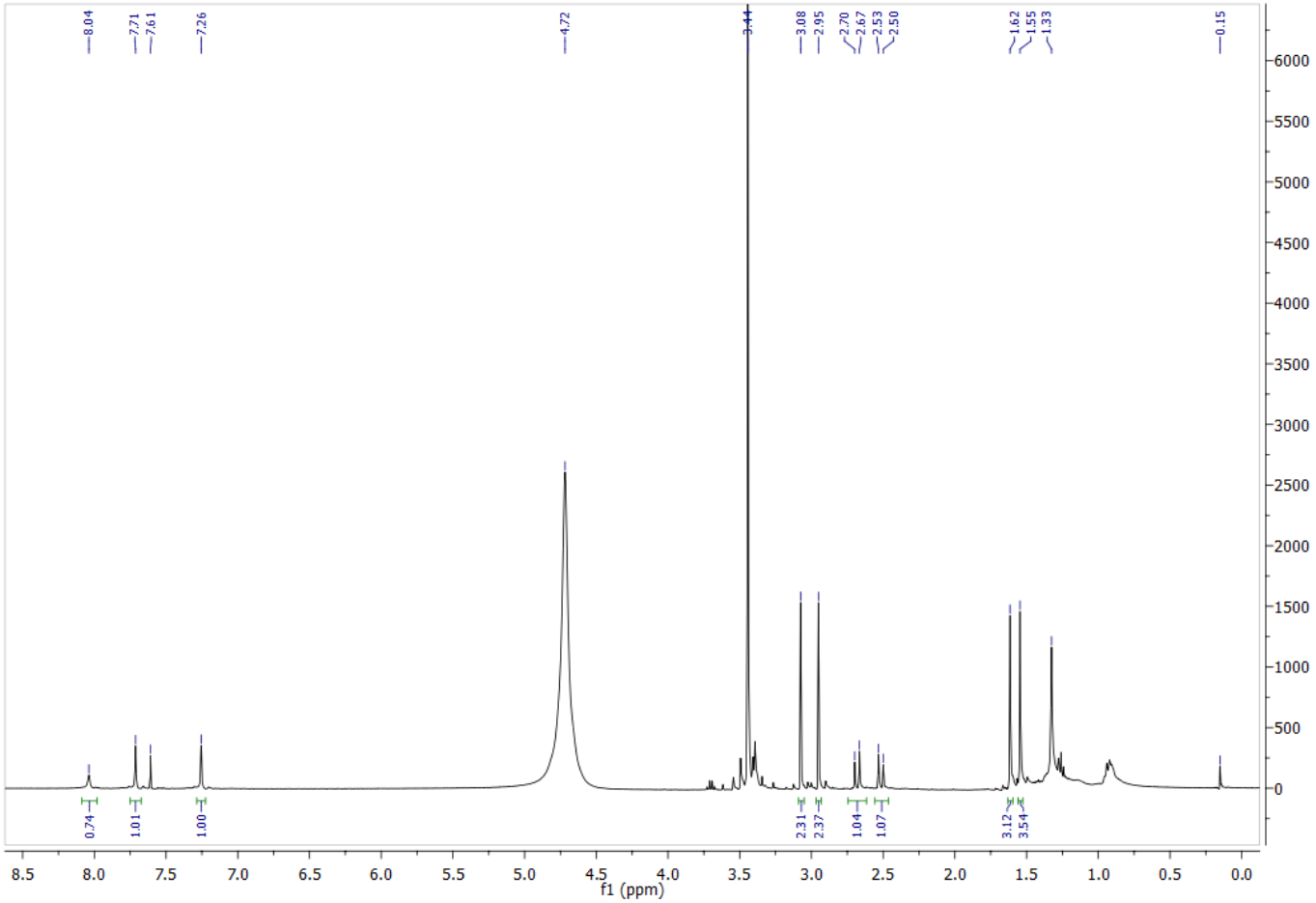

Figure S29: ^{1}H-NMR CFA-18 (400 MHz, $CDCl_3$, d_4-methanol, 49:1, 20°C).

In order to detect *spirta* in solution NMR-spectroscopy, the MOF has to be solved in acid (1M HCl) and the organic compounds were regained by extraction in chloroform. After washing and evaporating the solvent, a NMR-spectroscopy proves the intact linker molecule (*aR*-**7**) with a huge amount of DMF as a neutral ligand of the trigonal MAF-SBU.

Altogether, we demonstrated clearly, that *H_2-spirta* is included in the MOF-structure without any degradation at all.

4. Crystallographic data:

4.1. (aR)-3,3,3',3'-Tetramethyl-2,2',3,3'-tetrahydro-1,1'-spirobi[indene]-6,6'-diyl bis[(1R,2S,5R)-5-methyl-2-(propan-2-yl)cyclohexyl] biscarbonate (*aR*-2)

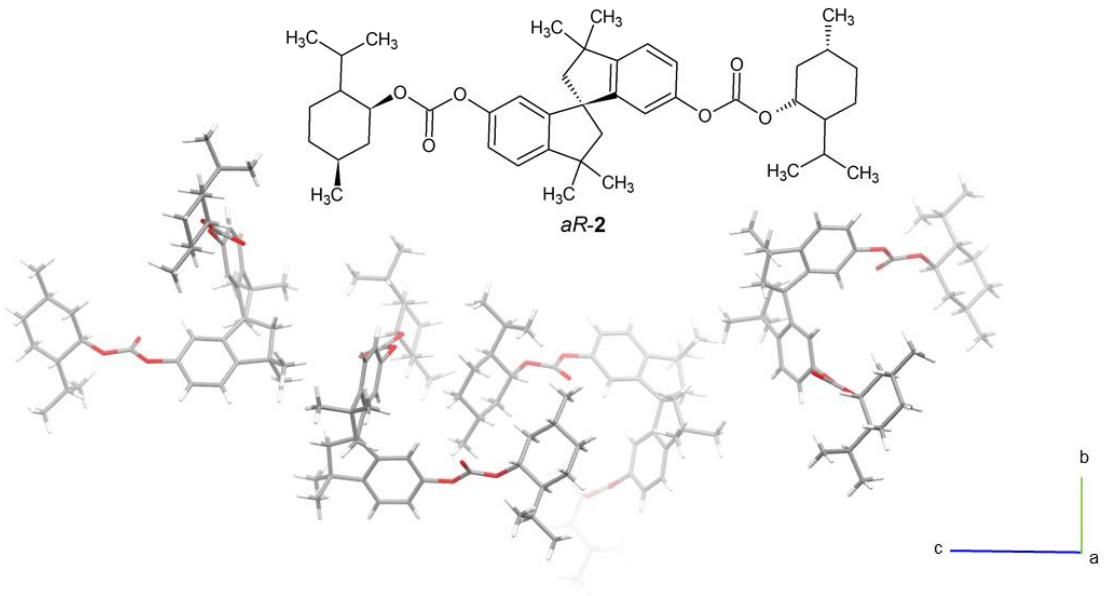

Figure S30: Crystal packing of *aR*-**2.**

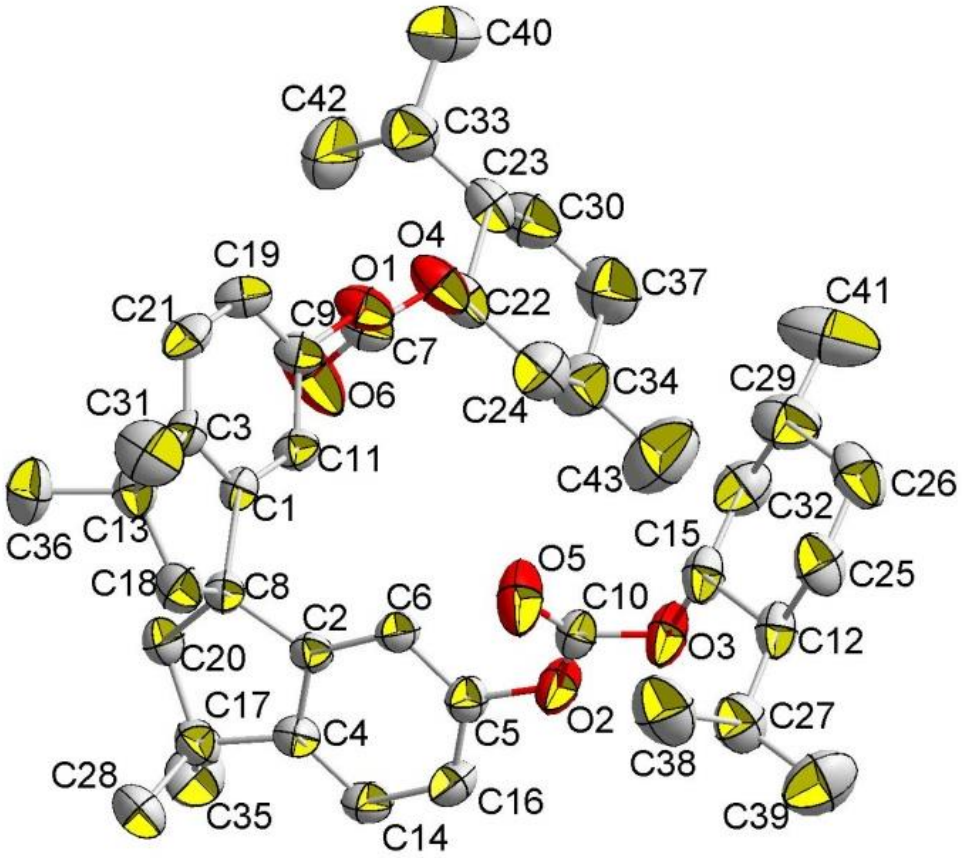

Figure S31: ORTEP-Style plot of asymmetric unit of compound *aR*-**2**. Thermal ellipsoids probability: 50%. Hydrogen atoms have been omitted for clarity.

Table S1. Crystal data and structure refinement for *aR*-**2**.

Identification code	CCDC2009789	
Empirical formula	C_{43} H_{60} O_6	
Formula weight	672.91	
Temperature	300(2) K	
Wavelength	0.71073 Å	
Crystal system	orthorhombic	
Space group	$P2_12_12_1$ (no. 19)	
Unit cell dimensions	a = 9.6730(5) Å	α= 90°.
	b = 10.5884(5) Å	β= 90°.
	c = 39.597(2) Å	γ = 90°.
Volume	4055.6(3) $Å^3$	
Z	4	
Density (calculated)	1.102 Mg/m^3	
Absorption coefficient	0.072 mm^{-1}	
F(000)	1464	
Crystal size	0.35 x 0.16 x 0.14 mm^3	
Theta range for data collection	2.181 to 28.181°.	
Index ranges	-13<=h<=13, -14<=k<=14, -53<=l<=53	
Reflections collected	239286	
Independent reflections	10542 [R(int) = 0.0782]	
Completeness to theta = 28.181°	99.9 %	
Refinement method	Full-matrix least-squares on F^2	
Data / restraints / parameters	10542 / 0 / 572	
Goodness-of-fit on F^2	1.100	
Final R indices [I>2sigma(I)]	R1 = 0.0624, wR2 = 0.1104	
R indices (all data)	R1 = 0.1086, wR2 = 0.1241	
Absolute structure parameter	0.10(17)	
Largest diff. peak and hole	0.249 and -0.168 e.$Å^{-3}$	

4.2. 3,3,3',3'-tetramethyl-5,5‘-dinitro-2,2',3,3'-tetrahydro-1,1'-spirobi[indene]-6,6'-diol (*rac*-4).

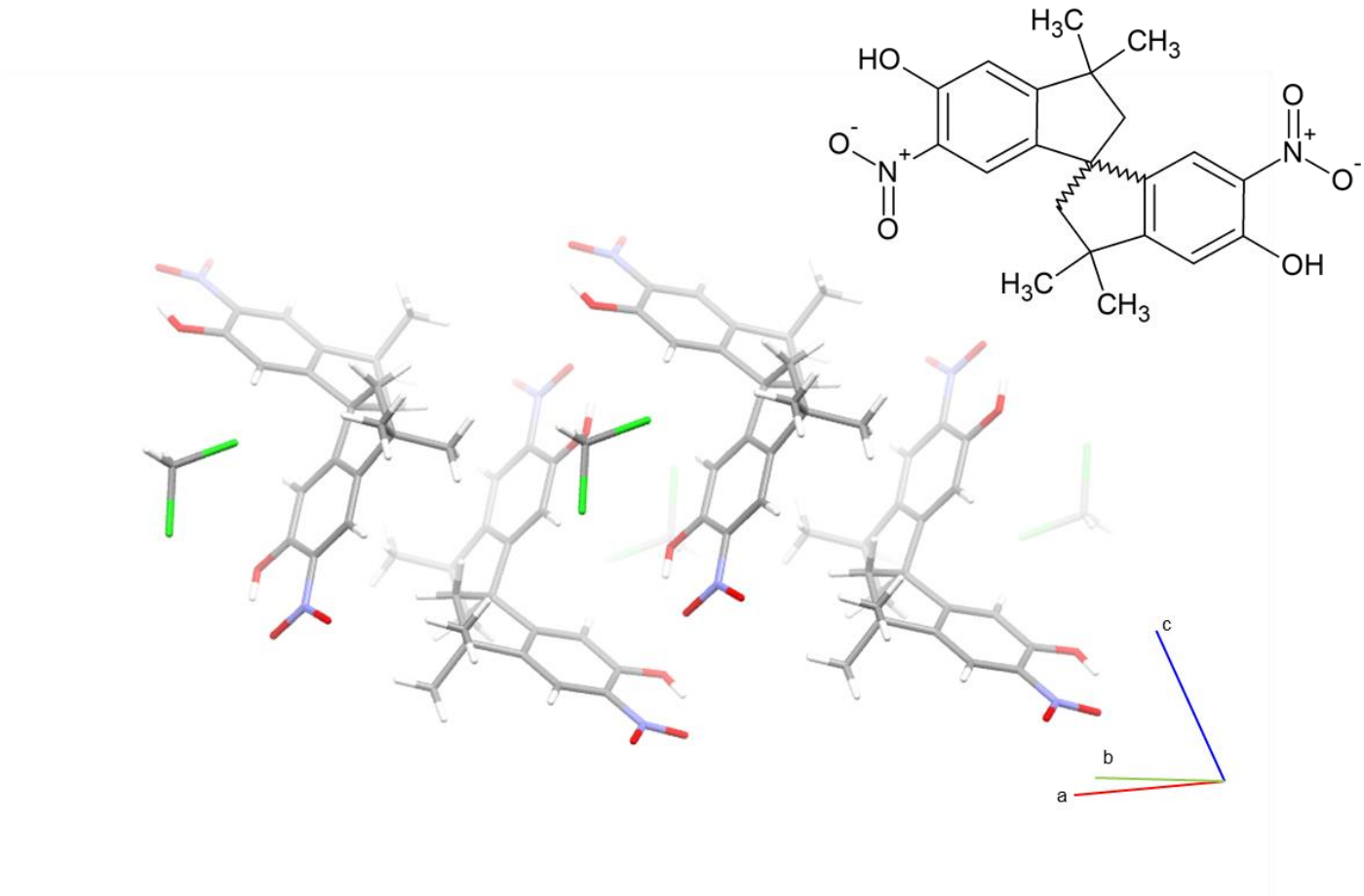

Figure S32: Crystal packing of *rac*-**4**.

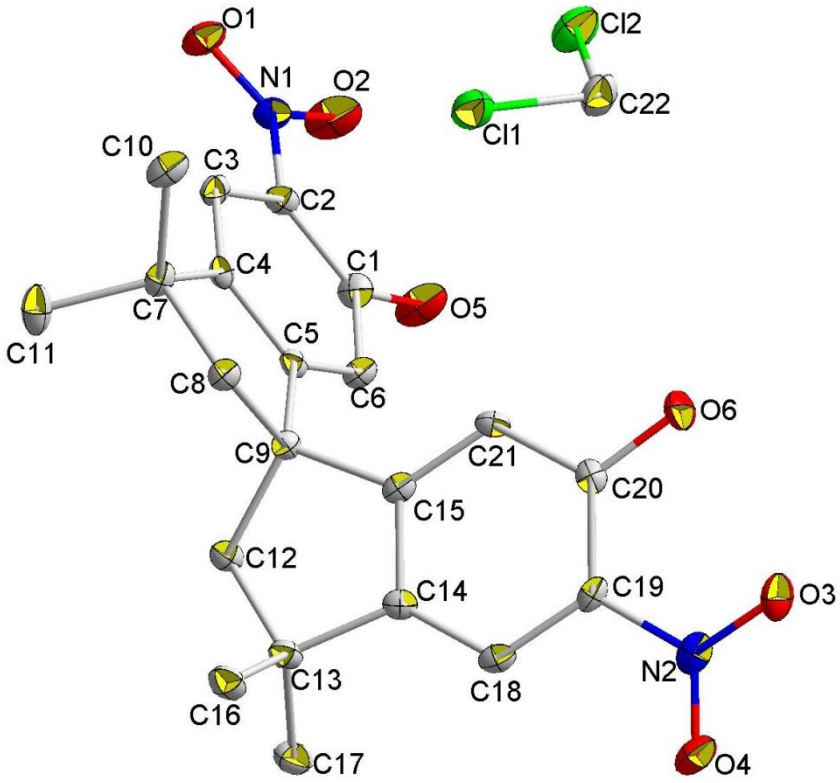

Figure S33: ORTEP-Style plot of asymmetric unit of compound *rac*-**4**. Thermal ellipsoids probability: 50%. Hydrogen atoms have been omitted for clarity.

Table S2. Crystal data and structure refinement for *rac*-**4**.

Identification code	CCDC2009786	
Empirical formula	C_{22} H_{24} Cl_2 N_2 O_6	
Formula weight	483.33	
Temperature	100(2) K	
Wavelength	0.71073 Å	
Crystal system	triclinic	
Space group	P-1	
Unit cell dimensions	a = 10.7580(3) Å	α= 67.7990(10)°.
	b = 10.9296(3) Å	β= 72.2600(10)°.
	c = 11.4620(4) Å	γ = 65.8980(10)°.
Volume	1120.83(6) $Å^3$	
Z	2	
Density (calculated)	1.432 Mg/m^3	
Absorption coefficient	0.332 mm^{-1}	
F(000)	504	
Theta range for data collection	2.11 to 26.11°.	
Index ranges	-13<=h<=13, -13<=k<=13, -14<=l<=14	
Reflections collected	31212	
Independent reflections	4463 [R(int) = 0.0639]	
Completeness to theta = 26.11°	99.8 %	
Refinement method	Full-matrix least-squares on F^2	
Data / restraints / parameters	4463 / 0 / 295	
Goodness-of-fit on F^2	1.040	
Final R indices [I>2sigma(I)]	R1 = 0.0389, wR2 = 0.0780	
R indices (all data)	R1 = 0.0597, wR2 = 0.0856	
Largest diff. peak and hole	0.353 and -0.222 $e.Å^{-3}$	

4.3. aR-3,3,3',3'-tetramethyl-5,5‘-dinitro-2,2',3,3'-tetrahydro-1,1'-spirobi[indene]-6,6'-diol (aR-4).

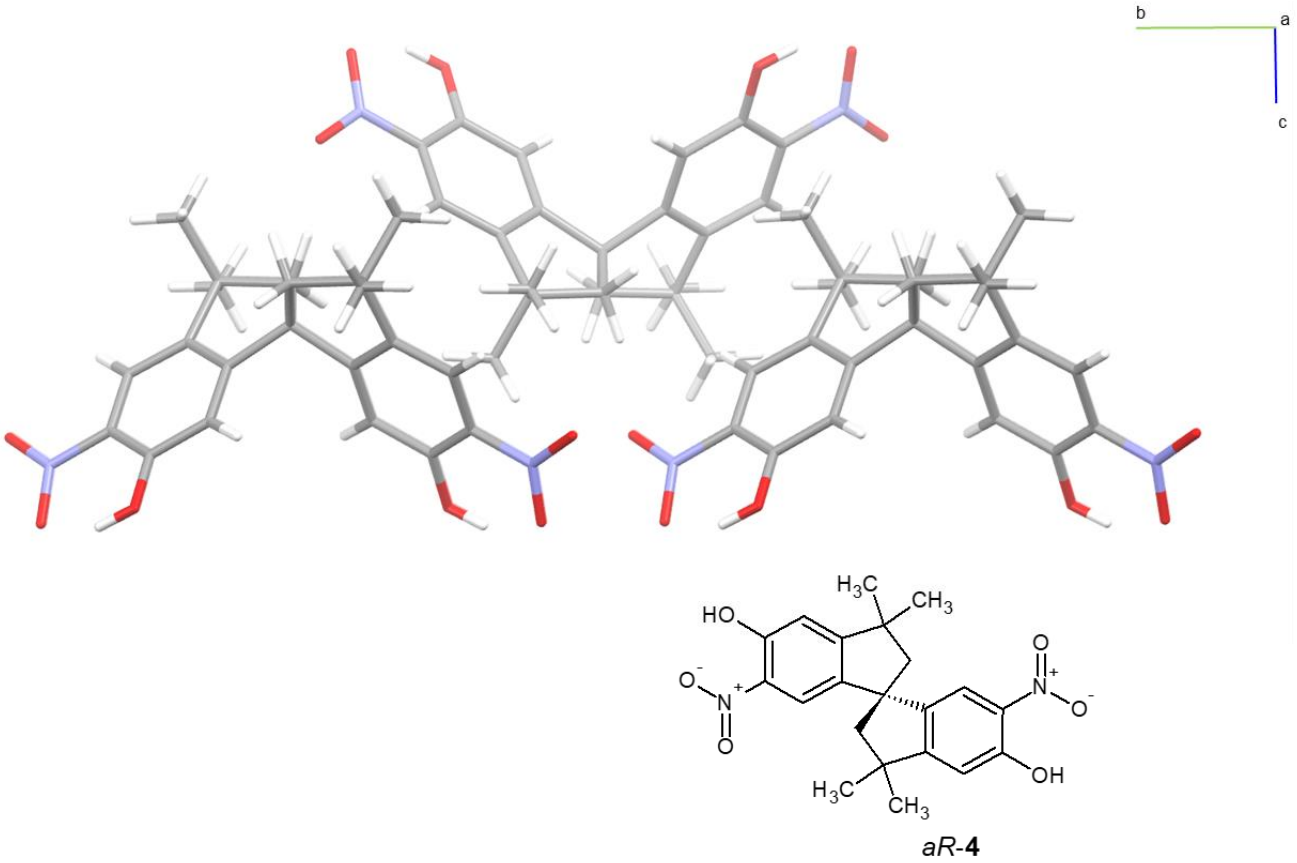

Figure S34: Crystal packing of *aR*-4.

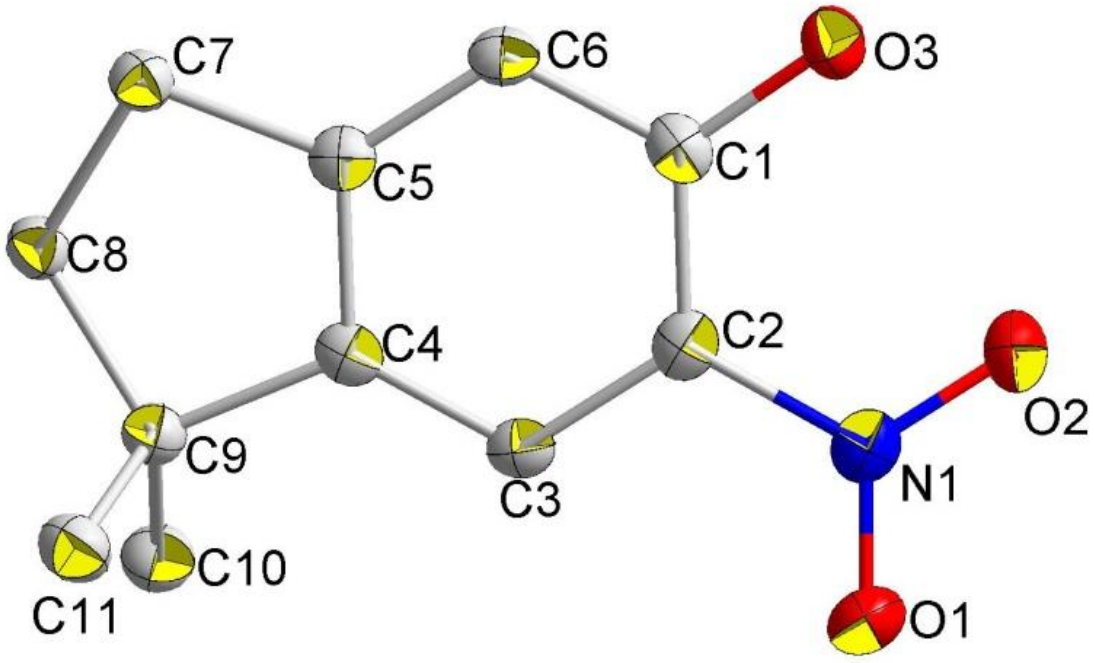

Figure S35: ORTEP-Style plot of asymmetric unit of compound *aR*-**4**. Thermal ellipsoids probability: 50%. Hydrogen atoms have been omitted for clarity.

Table S3. Crystal data and structure refinement for *aR*-**4**.

Identification code	CCDC2009785	
Empirical formula	C_{21} H_{22} N_2 O_6	
Formula weight	398.40	
Temperature	100(2) K	
Wavelength	1.54178 Å	
Crystal system	orthorhombic	
Space group	$P2_12_12$ (no. 18)	
Unit cell dimensions	a = 9.7978(3) Å	α= 90°.
	b = 12.4501(4) Å	β= 90°.
	c = 7.9839(3) Å	γ= 90°.
Volume	973.90(6) $Å^3$	
Z	2	
Density (calculated)	1.359 Mg/m^3	
Absorption coefficient	0.84 mm^{-1}	
F(000)	420	
Theta range for data collection	4.5 to 68.00°.	
Index ranges	-7<=h<=11, -14<=k<=14, -9<=l<=9	
Reflections collected	5274	
Independent reflections	1751 [R(int) = 0.023]	
Completeness to theta = 68.00°	98.7 %	
Refinement method	Full-matrix least-squares on F^2	
Data / restraints / parameters	1751 / 0 / 135	
Goodness-of-fit on F^2	1.089	
Final R indices [I>2sigma(I)]	R1 = 0.0310, wR2 = 0.0783	
R indices (all data)	R1 = 0.0328, wR2 = 0.0796	
Absolute structure parameter	-0.02(10)	
Largest diff. peak and hole	0.186 and -0.140 $e.Å^{-3}$	

4.4. aR-7,7,7',7'-tetramethyl-6,6',7,7'-tetrahydro-1H,3'H-5,5'-spirobi[indeno[5,6-d][1,2,3]triazole] (aR-7) - trigonal chiral space group $P3_12_1$

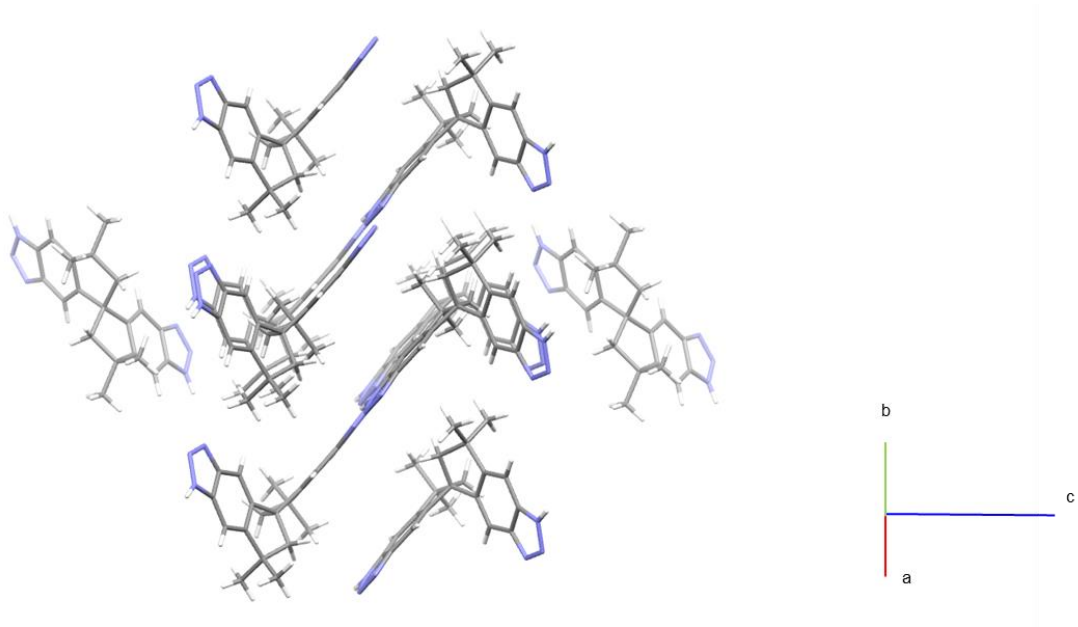

Figure S36: Trigonal crystal packing of *aR*-**7**.

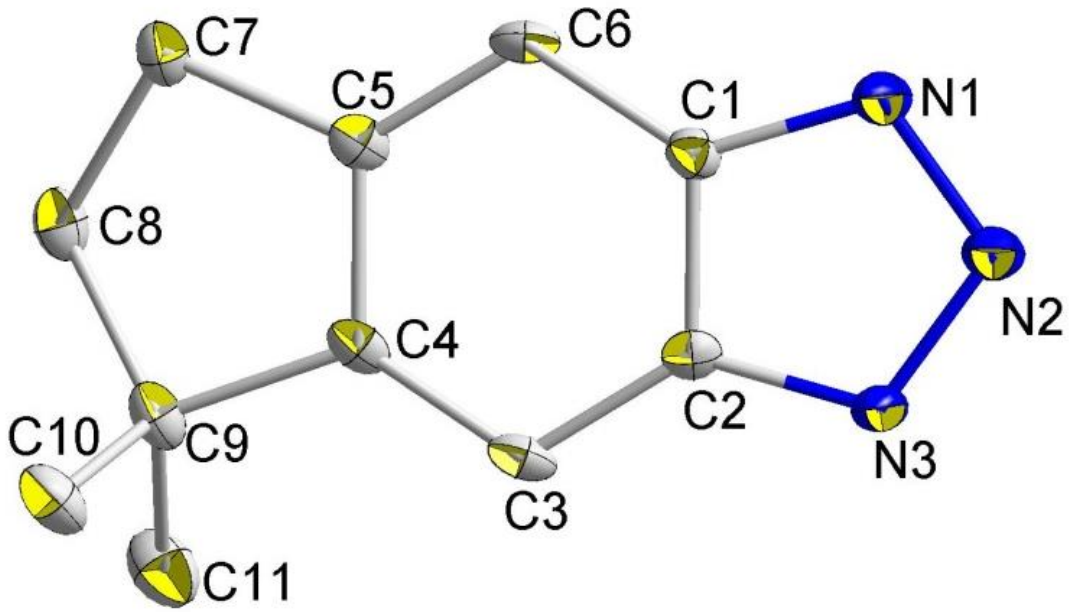

Figure S37: ORTEP-Style plot of asymmetric unit of compound *aR*-**7**. Thermal ellipsoids probability: 50%. Hydrogen atoms have been omitted for clarity.

Table S4: Crystal data and structure refinement summary of *aR*-**7** water free crystal.

Identification code	CCDC2009784	
Empirical formula	C_{21} H_{22} N_6	
Formula weight	358.44	
Temperature	100(2) K	
Wavelength	0.71073 Å	
Crystal system	Trigonal	
Space group	$P3_121$ (no. 152)	
Unit cell dimensions	a = 9.0638(3) Å	α= 90°.
	a = 9.0638(3) Å	β= 90°.
	c = 22.3036(9) Å	γ = 120°.
Volume	1586.81(12) $Å^3$	
Z	3	
Density (calculated)	1.125 Mg/m^3	
Absorption coefficient	0.07 mm^{-1}	
F(000)	570	
Crystal size	0.07 x 0.04 x 0.04 mm^3	
Theta range for data collection	2.6 to 25.00°	
Index ranges	-10<=h<=10, -10<=k<=10, -26<=l<=26	
Reflections collected	17089	
Independent reflections	1877 [R(int) = 0.092]	
Completeness to theta = 25°	100 %	
Refinement method	Full-matrix least-squares on F^2	
Data / restraints / parameters	1877 / 0 / 167	
Goodness-of-fit on F^2	1.13	
Final R indices [I>2sigma(I)]	R1 = 0.0540, wR2 = 0.0994	
R indices (all data)	R1 = 0.0680, wR2 = 0.1038	
Absolute structure parameter	0.6(10)	
Largest diff. peak and hole	0.18 and -0.21 $e.Å^{-3}$	

4.5. CFA-18

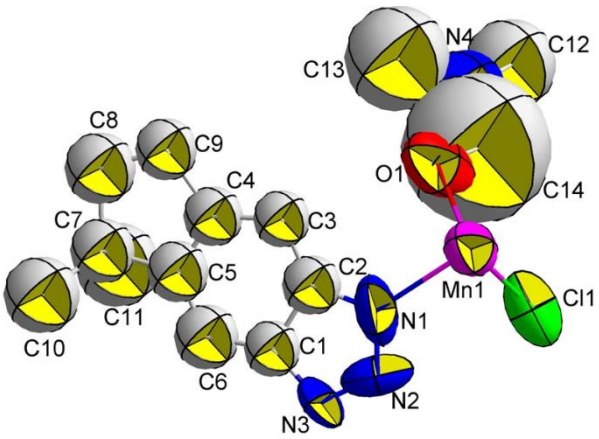

Figure S38: ORTEP-Style plot of asymmetric unit of CFA-18. Thermal ellipsoids probability: 50%. Hydrogen atoms have been omitted for clarity.

Table S5: Crystal data and structure refinement summary of CFA-18

Identification code	CCDC2009788
Empirical formula	$Mn_2Cl_2C_{27}H_{34}N_8O_2$
Formula	$Mn_2Cl_2C_{21}H_{20}N_6(C_3H_7NO)_2$
M_r/g mol^{-1}	683.40
T/K	100(2)
Wavelength/ Å	0.81040
Crystal system	trigonal
Space group	$P3_121$ (no.152)
a/Å	17.344(3)
c/Å	8.807(2)
V/Å^3	2294.5(9)
Z	3
D_c/g cm^{-3}	1.484
μ/mm^{-1}	1.495
F(000)	1056
Crystal size/mm^3	0.03 x 0.01 x 0.005
Θ range/°	2.637 to 27.481
Refl. collected	22416
Refl. unique	2365
Completeness to theta = 27.481°/%	99.9
Data / restraints / parameters	2365 / 11 / 115
R(int)	0.1139
GooF	1.003
Final R indices [I>2sigma(I)][a]	R1 = 0.0999, wR2 = 0.2540
R indices (all data)[b]	R1 = 0.1607, wR2 = 0.3084
Flack parameter	0.04(3)
Largest diff. peak and hole/ e.Å^{-3}	0.455 and -0.444

a $R_1 = \sum||Fo| - |Fc||/\sum|Fo|$. b $wR_2 = \sum[w(F_o^2 - F_c^2)2]/\sum[w(F_o^2)2]^{1/2}$.

Table S6: Comparison of selected bond lengths [Å] for **CFA-18** and MAF[3].

	$[MnCl_2(spirta)_2(DMF)_2]$ (CFA-18)	$[MnCl_2(BBTA)_2(H_2O)_2]$ (MAF-X25)
Mn1-N1	2.32(2)	2.241(3)
Mn1-N2	2.26(2)	2.275(4)
Mn1-N3	2.28(2)	n/a
Mn1-Cl1	2.53(1)	2.5209(9)
Mn1-O1	2.17(2)	2.303(4)

5. Gas Adsorption measurement:

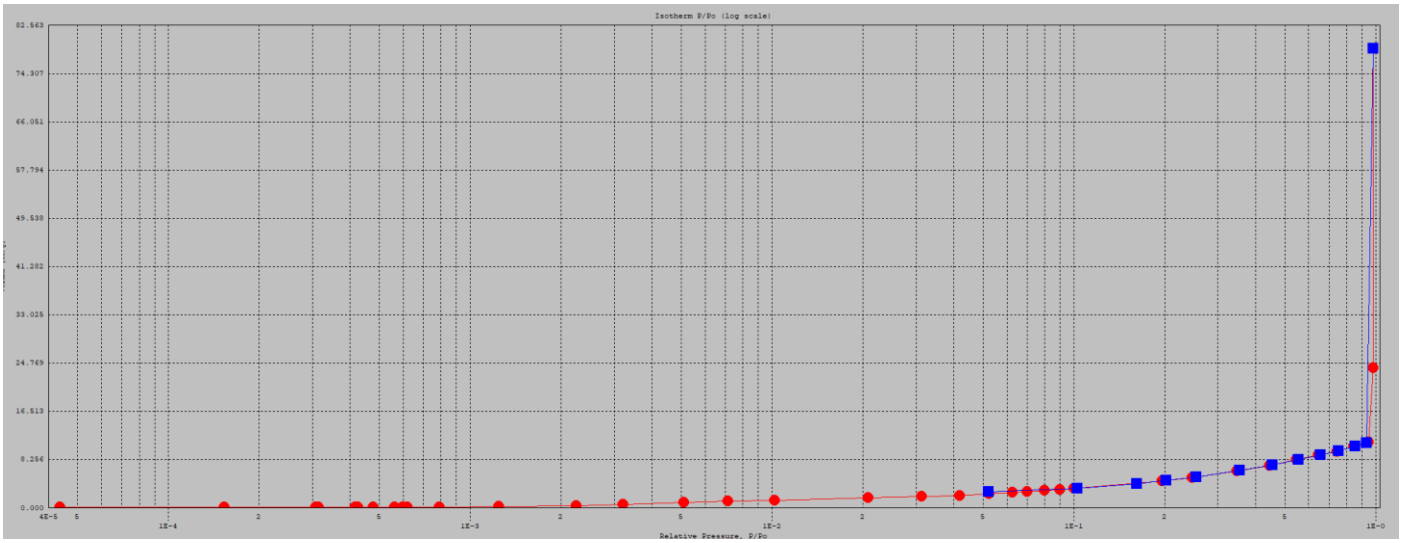

Figure S39: Gas adsorption measurement with argon at 77 K. BET fitting gives a surface area of 17 m²/g.

References

1 J. Rubim, I.G.R. Gutz, O. Sala and W. J. Orville-Thomas, *J. Mol. Struct.*, 1983, **100**, 571–583.

2 S. Biswas, M. Tonigold, M. Speldrich, P. Kögerler, M. Weil and D. Volkmer, *Inorg. Chem.*, 2010, **49**, 7424–7434.

3 P.-Q. Liao, X.-Y. Li, J. Bai, C.-T. He, D.-D. Zhou, W.-X. Zhang, J.-P. Zhang and X.-M. Chen, *Chem. Eur. J.*, 2014, **20**, 11303–11307.